Article

An Optimized Glutamate Receptor Photoswitch with Sensitized Azobenzene Isomerization

Marta Gascón-Moya, Arnau Pejoan, Mercè Izquierdo-Serra, Silvia Pittolo, Gisela Cabrè, Jordi Hernando, Ramon Alibés, Pau Gorostiza, and Felix Busque

J. Org. Chem., **Just Accepted Manuscript** • DOI: 10.1021/acs.joc.5b01402 • Publication Date (Web): 28 Sep 2015

An Optimized Glutamate Receptor Photoswitch with Sensitized Azobenzene Isomerization

*Marta Gascón-Moya,[a] Arnau Pejoan,[a] Mercè Izquierdo-Serra,[b] Silvia Pittolo,[b] Gisela Cabré,[a] Jordi Hernando,[a] Ramon Alibés,[a] Pau Gorostiza,[b,c,d] * Félix Busqué [a] **

[a] Departament de Química, Universitat Autònoma de Barcelona, 08193 Bellaterra, Spain

[b] Institut de Bioenginyeria de Catalunya (IBEC), Barcelona, Spain

[c] Centro de Investigación Biomédica en Red en Bioingeniería, Biomateriales y Nanomedicina (CIBER-BBN), Zaragoza, Spain

[d] Institució Catalana de Recerca i Estudis Avançats (ICREA), Barcelona, Spain

pau@icrea.cat, felix.busque@uab.es

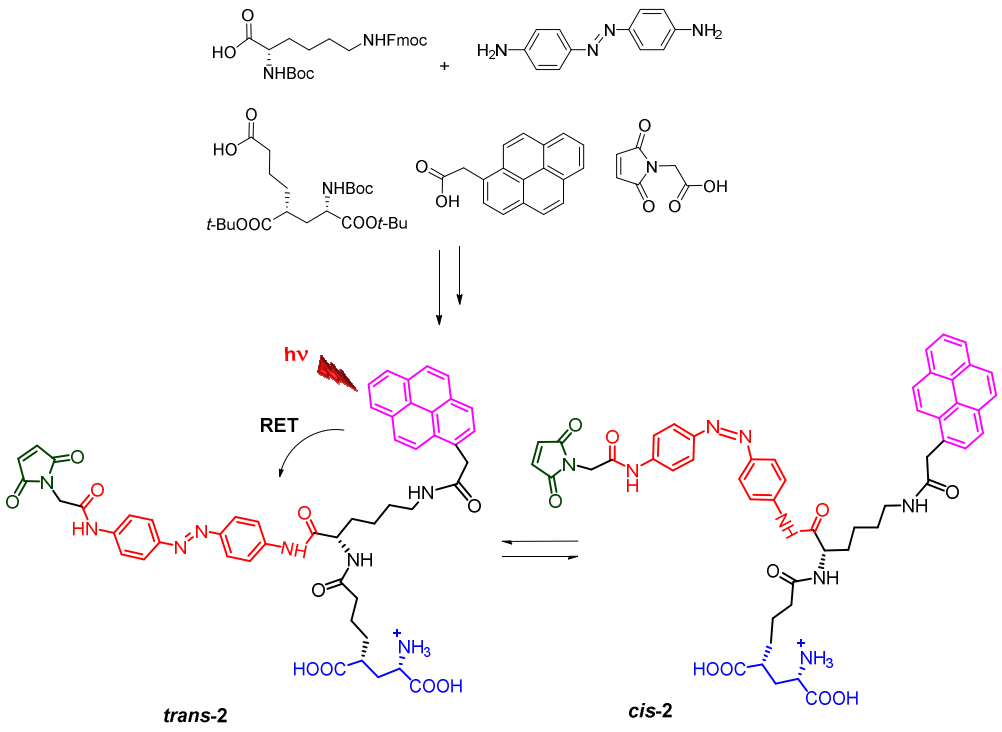

Abstract

A new azobenzene-based photoswitch, **2**, has been designed to enable optical control of ionotropic glutamate receptors in neurons via sensitized two-photon excitation with NIR light. In order to develop an efficient and versatile synthetic route for this molecule, a modular strategy is described which relies on the use of a new linear fully protected glutamate derivative stable in basic media. The resulting compound undergoes one-photon *trans*-*cis* photoisomerization via two different mechanisms: direct excitation of its azoaromatic unit, and irradiation of the pyrene sensitizer, a well known two-photon sensitive chromophore. Moreover, **2** presents large thermal stability of its *cis* isomer, in contrast to other two-photon responsive switches relying on the intrinsic non-linear optical properties of push-pull substituted azobenzenes. As a result, the molecular system developed herein is a very promising candidate for evoking large photoinduced biological responses during the multiphoton operation of neuronal glutamate receptors with NIR light, which require accumulation of the protein-bound *cis* state of the switch upon repeated illumination.

Introduction

Neuroscience is being revolutionized in the last years by the emergence of optogenetic[1] and optochemical tools,[2] a series of techniques that allow the optical control of neural networks by means of light-sensitive proteins and photoresponsive small molecules. An important strategy in this field is the use of photoswitchable tethered ligands (PTLs), in which a pharmacologically active moiety is covalently attached to a neuronal receptor through a photoisomerizable tether.[2,3] This enables the activity of the resulting protein-PTL construct to be modulated upon photoisomerization of the switch, which brings the ligand closer to or away from the binding site and, as such, triggers a reversible light-induced recognition event and the subsequent biological response. Owing to their synthetic accessibility, excellent photochemical properties and large geometrical change between their photointerconvertible *trans* and *cis* configurations, azobenzene derivatives have become the most common light-responsive

building blocks for the preparation of PTLs[4] and they have been exploited to optically control a number of different neuronal receptors.2[,3,5]

Since glutamate is the major excitatory neurotransmitter in the central nervous system, glutamate receptors play a central role in the regulation of neural activity[6] and are an important target of optochemical techniques. Much attention has therefore been focused in recent years on the development of PTLs for the light-induced operation of these proteins, especially in the case of the ionotropic glutamate receptors (iGluR) controlling the channel-regulated flow of ions through cell membrane.[2,3] The most successful approach towards this goal is based on maleimide-azobenzene-glutamate photoswitches (MAG, Figure 1a),[7] which were originally designed to enable optical control of the kainate-type ionotropic glutamate receptor GluK2. In MAG compounds, a lateral maleimide unit is used to covalently bind the PTL to a cysteine residue genetically engineered into the ligand binding domain of the receptor, while its photoswitchable azobenzene core enables light-control of the separation distance between the glutamate moiety and the binding pocket. In particular, *trans*-to-*cis* isomerization of the system approaches the ligand towards the binding site and induces glutamate recognition, which leads to ion channel opening and, eventually, to the generation of a photoinduced neuronal excitatory potential (Figure 1b).[7] Afterward, irradiation or thermal relaxation of the metastable *cis* isomer allow reverting back the process and recovering the initial closed state of the channel.[7] For the first MAG switch developed (Figure 1a), irradiation with UV-violet ($\lambda_{trans\text{-}cis}$ ~ 340-400 nm) and blue-green light ($\lambda_{cis\text{-}trans}$ ~ 440-580 nm) were required to photochemically operate the tagged GluK2 receptors,[7] while spontaneous *cis*-to-*trans* isomerization occurred in the dark on the minute time scale (τ_{cis}= 17.7 min)[7b] owing to the large thermal stability of the *cis* isomer resulting from its symmetric 4,4'-diamide substitution pattern.[4] Although some efforts have been devoted to shift MAG photoactivity to longer wavelengths,[8,9] the application of these compounds *in vivo* is severely compromised by the reduced penetration depth[10] and low axial resolution associated to the conventional one-photon excitation of azobenzene-based switches with UV-visible light. To overcome these drawbacks and take full

advantage of the light-regulated activity of MAG-labeled receptors, multiphoton excitation with near-infrared (NIR) light would be highly desirable, since it provides sub-micrometric resolution in three dimensions,[11] deep penetration into tissue[12] and patterned illumination.[13,14] Unfortunately, the two-photon absorption cross-sections of common azobenzene chromophores are rather low,[15] which makes multiphoton operation of MAG PTLs under NIR irradiation a challenge.

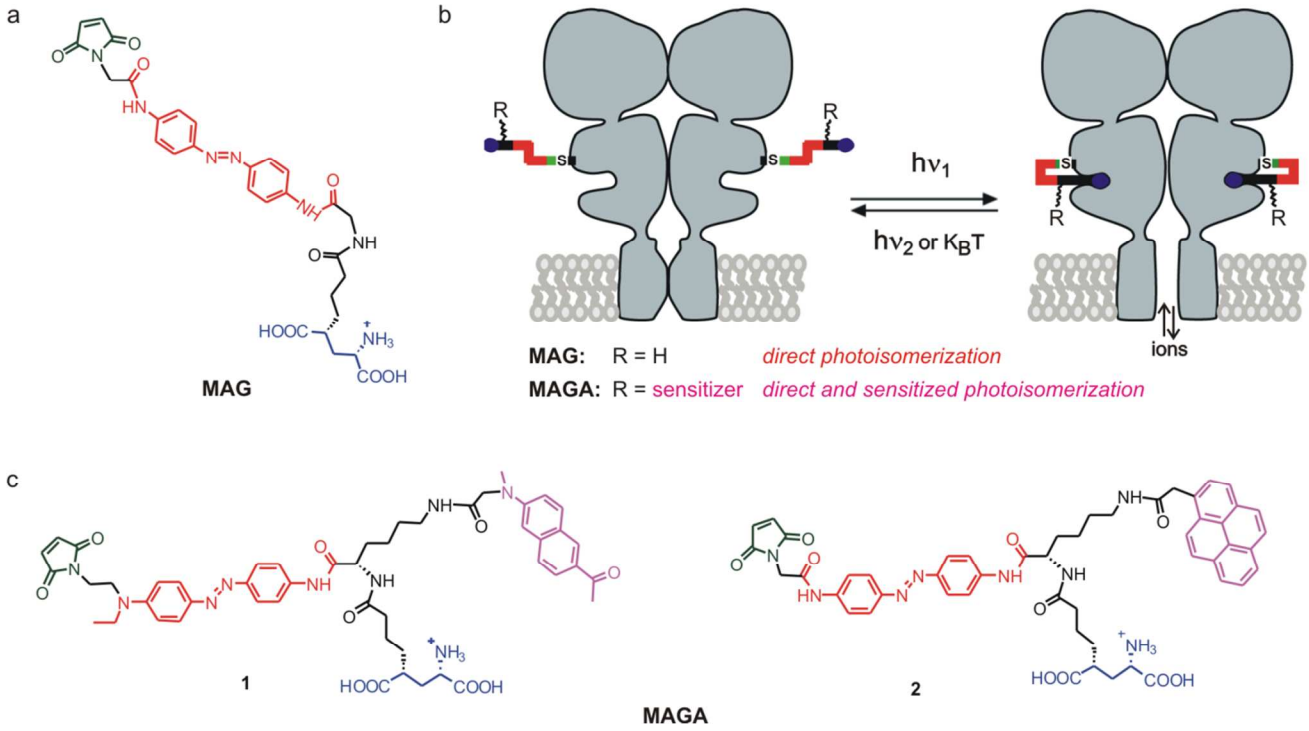

Figure 1. (a) Structure of a MAG molecular switch composed of maleimide (green), azobenzene (red) and glutamate (blue) units.7 (b) Operation mode of a cysteine-tagged ionotropic glutamate receptor functionalized with a photoswitchable tethered ligand. Reversible isomerization of the azoaromatic core of the switch modulates the separation distance between the glutamate ligand and the binding site of the receptor to induce channel opening (*trans*-to-*cis*) and closing (*cis*-to-*trans*). In this work, an additional building block is introduced into the structure of the PTL, an antenna enabling two-photon sensitization of azobenzene isomerization (MAGA-type switch). (c) Structures of the MAGA photoswitched tethered ligands **1** and **2**, whose additional sensitizer unit is shown in magenta.

To tackle this problem, we have recently introduced two different molecular strategies, which allowed for the first time the two-photon optical control of light-gated ionotropic glutamate receptors based on cysteine-tagged GluK2 and MAG switches (LiGluR-MAG).[16] On the one hand, the intrinsic two-photon activity of MAG compounds was shown to significantly increase upon push-pull substitution of their azobenzene core, as subsequently demonstrated by Isacoff and co-workers for analogous PTLs.[17] However, a decrease of the thermal stability of the *cis* state of these systems was concomitantly observed,[16,17] which imposes a severe constraint on their photochemical behavior: the ligand-bound state of the LiGluR-MAG tether dissociates as soon as illumination ceases, since the *cis* liganding configuration of the switch back-isomerizes in the dark on the ms scale. While this might be advantageous for certain applications requiring fast operation of ionotropic glutamate receptors,[16] rapid thermal relaxation of the switch prevents building up a large population of the open state of the ion channel and, therefore, the obtaining of large photoresponse amplitudes. Alternatively, multiphoton operation of MAG-type PTLs can be attained by incorporating a photosensitizer unit to the structure of the switch, which should absorb NIR light via a two-photon process and efficiently transfer its electronic excitation energy to the azobenzene chromophore (Figure 1b). We named this new family of compounds maleimide-azobenzene-glutamate-antenna switches (MAGA),[16] whose multiphoton response could then be disentangled from the substitution pattern of the azoaromatic core. Actually, the one- and two-photon sensitized isomerization of a MAGA-type PTL was already demonstrated in our previous work using a naphthalene antenna (**1** in Figure 1c); however, this compound also suffered from low *cis* thermal stability owing to the push-pull substitution of the azobenzene core selected (τ_{cis} = 265 ms at 298 K) and, consequently, displayed reduced multiphoton activity when conjugated to LiGluR.[16] In view of this, we pursue herein the preparation of a new MAGA photoswitch featuring both sensitized isomerization using a two-photon absorber and long *cis* state lifetime in the dark. As such, this compound could be exploited to optically trigger the LiGluR receptor via multiphoton absorption of NIR light in neuroscience applications demanding large biological photoinduced signals (i.e. accumulation of the open state of the channel upon repeated excitation).

Figure 1c shows the structure of **2**, the novel MAGA-type PTL targeted in this work. This compound was derived on account of two main design concepts. First, the use of a symmetrically substituted azobenzene chromophore displaying two similar *N*-amido substituents at positions 4 and 4', which should ensure a long thermal lifetime of its *cis* state at room temperature according to the previous results obtained for MAG[7] and other related azoaromatic derivatives.[18] Second, the selection of a proper multiphoton antenna, which should (i) display large two-photon absorption under NIR irradiation, and (ii) emit in the same spectral region where the azobenzene core absorbs, thus enabling efficient sensitization of the switch via resonance energy transfer (RET). Since the 4,4'-diamidoazobenzene core in **2** must present a large hypsochromic absorption shift with respect to the azoaromatic group of **1** (~70 nm),[7,16,18] the naphtalene sensitizer of the latter compound did not fulfil the second of the requirements of our present design and could not be used as antenna for the development of switch **2**. Instead, a mono-alkylated pyrene derivative was chosen as sensitizer. Although this type of dyes present moderate two-photon absorption cross-sections,[19] they are often used as two-photon fluorescent probes for labeling cell membranes in confocal fluorescence microscopy studies[18] and can be detected even down to the single-molecule level under two-photon excitation.[20] More importantly, their emission spectra ($\lambda_{fl,max}$ ~ 390 nm[19]) largely overlaps the absorption spectra of the $\pi \rightarrow \pi^*$ transition of *trans*-4,4'-diamidoazobenzenes ($\lambda_{abs,max}$ ~ 370 nm[18]), a critical requirement for photosensitization of their *trans*-to-*cis* isomerization.

Results and Discussion

Synthesis of photoswitchable ligand 2

A convergent synthetic strategy was devised for the preparation of **2**, which relies on the use of five different building blocks (Scheme 1): the *N*,*N*-orthogonally diprotected L-lysine **3**; *trans*-4,4'-diaminoazobenzene (**4**) as the symmetrically-substituted azoaromatic core; the linear protected derivative of glutamate **5**; 2-(pyren-1-yl)acetic acid (**6**) as two-photon sensitizer; and maleimide

derivative **7**. Two key features differentiate our approach from the synthetic procedures previously reported for the synthesis of analogous MAG photoswitches.[7-9] On the one hand, the use of **3** as a central scaffold to which the distinct functional fragments of the target compound would be sequentially tethered, thus aiming to develop a modular route toward MAGA PTLs (or any other type of multifunctional ligand derived from the original maleimide-azobenzene-glutamate scheme). On the other hand, **5** was developed as an alternative glutamate precursor to typical cyclic pyroglutamate groups, providing an optimized strategy to achieve the final photoswitchable ligand in terms of both deprotection reaction conditions and intermediate manipulation.

Scheme 1. Retrosynthetic analysis proposed for the synthesis of new MAG compound **2**

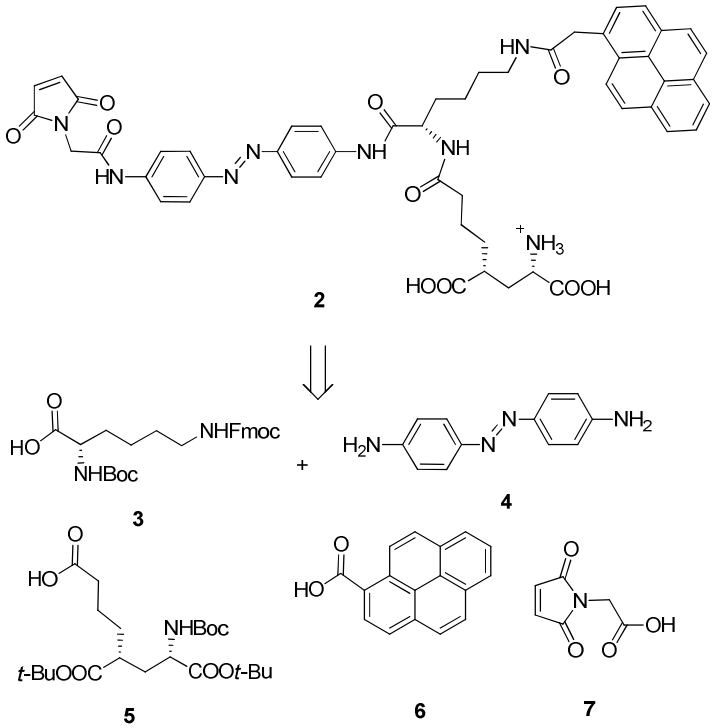

Since all the other building blocks of **2** were commercially available or synthetically accessible via prior reported procedures, our initial task focused on the preparation of glutamate derivative **5**. Although this compound has been recently used by us for the synthesis of **1**,[16] we describe herein the obtaining of **5** for the first time. The synthetic sequence commenced with the protection of the carboxylic acid and

the nitrogen atom of commercial L-piroglutamic acid as the corresponding *tert*-butyl ester and *tert*-butyl carbamate, respectively, to obtain known pyroglutamate **8**[21] in a 53% overall yield (Scheme 2). Next, this product was treated with LiHMDS in THF at – 78 ºC to form the corresponding enolate, which was allowed to react with allyl bromide at low temperature to afford a 3:1 diastereoisomeric mixture of already described allylated derivatives *trans* **9a** and *cis* **9b**.[22] The major *trans* diastereoisomer **9a** was isolated after purification by column chromatography in a 36% yield and used in the following steps of the synthesis. The relative configuration assignment of these two isomers was confirmed by comparison with the described NMR data.[22] Thus, in the ^{1}H NMR spectrum of **9a** H-2 resonates at an upper field than that of **9b** and shows constant couplings with H-3 protons quite different (9.6 and 1.6 Hz), whereas the values of these constants are more similar in the *cis* isomer (9.3 and 5.7 Hz).

Scheme 2. Synthesis of key intermediate **9a**

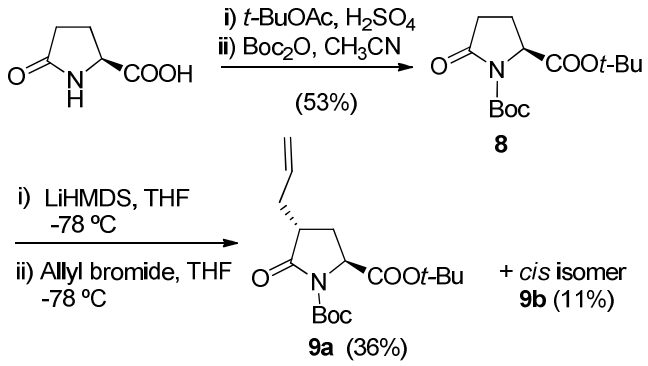

Subsequent lithium hydroxide ring opening of **9a** proceeded smoothly providing acid **10** in 93% yield (Scheme 3), which was transformed into the corresponding di-*tert*-butyl ester derivative **11** in 56% yield by treatment with *tert*-butyl 2,2,2,-trichloroacetimidate in the presence of catalytic BF_3. The synthesis was continued with a cross-metathesis reaction of **11** with crotonaldehyde using the Hoveyda-Grubs second generation catalyst to afford aldehyde **12** in 89% yield, which was oxidized to the corresponding acid **13** in 77% yield following a Pinnick protocol with $NaClO_2$ in the presence of 2-methyl-2-butene as scavenger of the hypochlorous acid generated. Direct metathesis reaction of intermediate **11** with acrylic

acid afforded derivative **13** in lower yield (52%) than that obtained with the two consecutive transformations described above (69% overall yield for the two steps). Finally, standard hydrogenation under palladium catalyst rendered almost quantitatively the target glutamate derivative **5**.

Scheme 3. Synthesis of glutamate derivative **5**

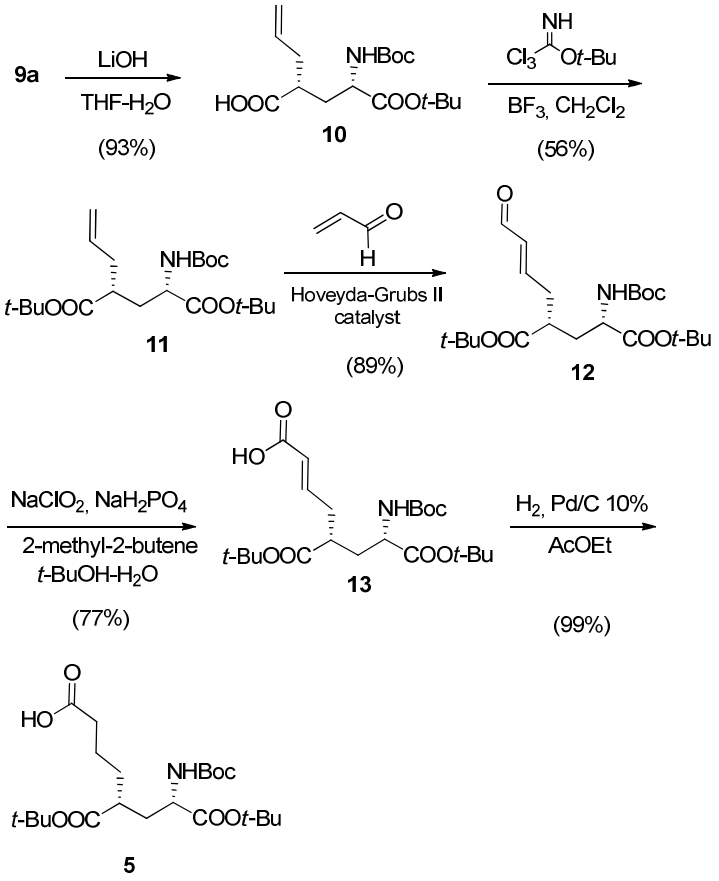

With glutamate derivative **5** in hand, we proceeded to prepare the final MAGA photoswitch **2** (Scheme 4) following the modular synthetic strategy outlined above and previously implemented in our group for the obtaining of **1**.[16] Accordingly, the *N*,*N*-orthogonally diprotected L-lysine **3** was tethered to the symmetric azobenzene core **4** using the carbodiimide coupling reagent EDCI along with HOBt and DIPEA as base, which led to a chromatographically easily separable mixture of starting material and compound **14** in 85% yield (over consumed starting material). Removal of the *tert*-butyl carbamate protection of this compound by treatment with 37% HCl in MeOH for 1 hour furnished amine **15** in

98% yield. Longer reaction times led to partial hydrolysis of the amide moiety and should be strictly avoided. Next, the glutamate derivative **5** was introduced into this intermediate using again EDCI under standard coupling conditions, affording derivative **16** in 88% yield. The incorporation of the pyrene sensitizer was then achieved by treatment of **16** with 20% piperidine solution in DMF to render the corresponding reactive amine **17** and successive EDCI-promoted amide formation with **6**. In this way, **18** was obtained in 64% overall yield for the two steps. The subsequent reaction between this intermediate and the freshly made acid chloride of maleimide derivative **7**[23] afforded compound **19** in 74% yield, which features all the functional fragments of the final MAGA switch.

Scheme 4. Synthesis of the new MAGA compound **2**

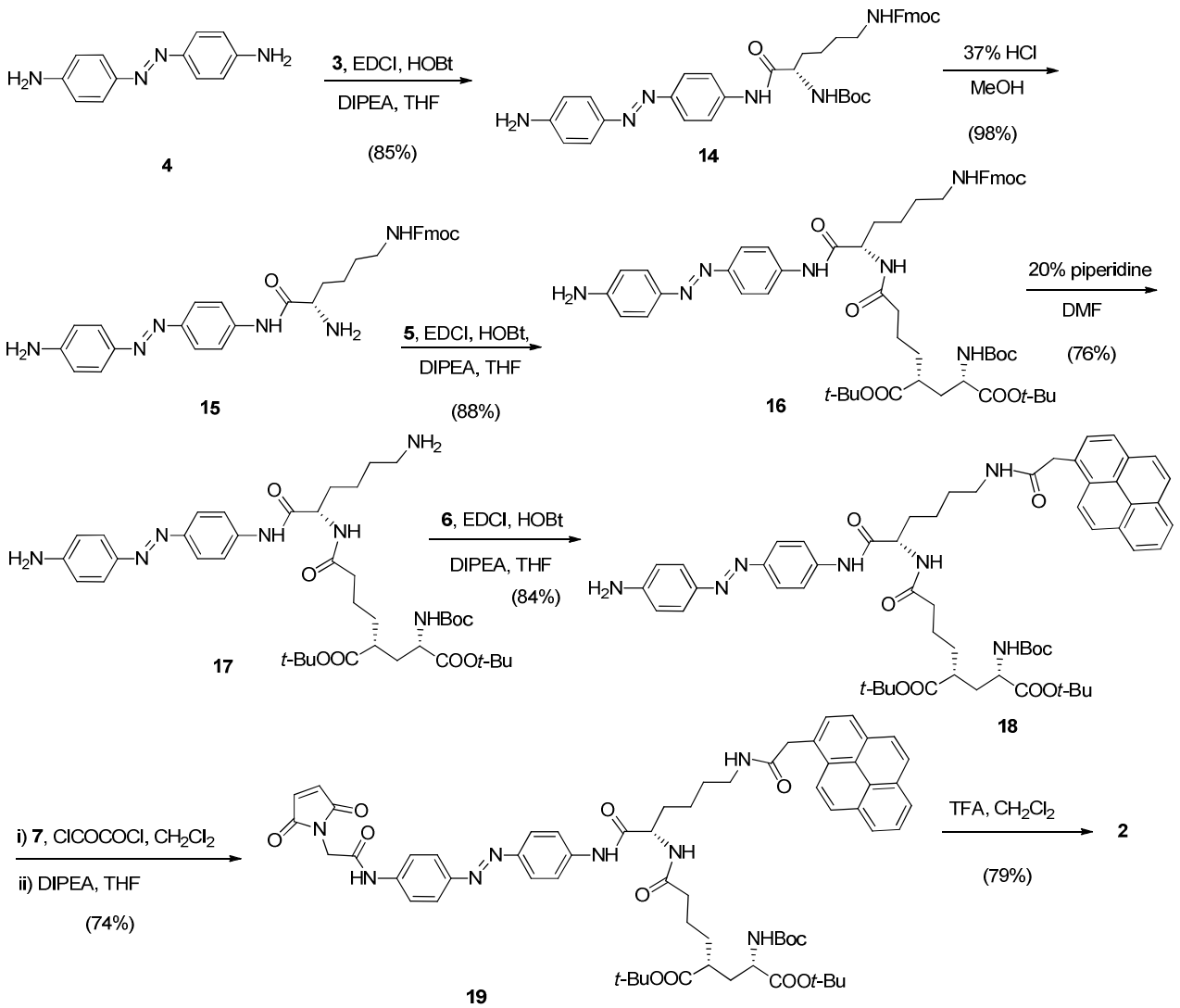

The preparation and manipulation of such advanced intermediate was highly favored by the use of the new linear glutamate derivative **5**. In our hands, **5** turned to be a better glutamate precursor than the cyclic pyroglutamate group normally employed in the synthesis of MAG compounds,[7-9] which we found to be troublesome due to: (i) the moderate stability to the basic conditions required for the ring opening reaction of pyroglutamate of the maleimide fragment, which should therefore be introduced in a later stage of the route; and (ii) the low solubility of the dicarboxylic acid generated from the ring opening process of the pyroglutamate precursor,[7-9] which compromised its manipulation and the efficiency of posterior reactions (e.g. incorporation of the maleimide group). These inconveniences are overcome by the use of the already opened derivative of glutamate **5** whose carboxylic acid groups are protected as the corresponding *tert*-butyl esters. Finally, removal of these moieties and of the additional *tert*-butyl carbamate protecting group of intermediate **19** took place in a single final step by treatment with a 2:1 mixture of trifluoroacetic acid and CH_2Cl_2, thus providing the monotrifluoroacetate salt of target ligand **2** in 79% yield. As expected, this compound was selectively isolated as its more stable *trans* isomer (*trans*-**2**), according to spectroscopic data.

One-photon optical characterization of photoswitchable ligand 2

Aiming to assess the validity of our molecular design, the optical properties of compound **2** were investigated to demonstrate both sensitization of the *trans*-*cis* isomerization of the ligand upon photoexcitation of the pyrene antenna and the long thermal stability of the *cis* state of the switch at room temperature. For sake of simplicity, this study was conducted under one-photon excitation with UV-vis light. However, based on our previous work[16] and the well known non-linear optical properties of pyrene derivatives,[19-20] the results obtained herein could be extrapolated to the photochemical behavior expected for **2** upon two-photon absorption of NIR light.

Figure 2a shows the absorption spectrum of *trans*-**2** in DMSO, which is compared to those recorded for its photoactive building blocks: pyrene derivative **6** and *trans*-4,4'-bis(acetylamino)azobenzene

(*trans*-**20**), a model azoaromatic dye obtained by bis-acylation of 4,4'-diaminoazobenzene using standard amide formation conditions according to literature precedents.[24] Clearly, the narrow pyrene vibronic absorption peaks at λ_{abs} ~ 315, 330 and 345 nm and the broad *trans*-azoaromatic $\pi \rightarrow \pi^*$ ($\lambda_{abs,max}$ = 380 nm) and $n \rightarrow \pi^*$ ($\lambda_{abs} > 450$ nm) absorption bands are both observed in the spectrum of *trans*-**2**. This does not only demonstrate the successful introduction of the two chromophoric units, but also that they are not electronically coupled in the ground state of the ligand. In contrast, non-negligible interactions should take place in the electronic excited state, as revealed by the fluorescence emission spectra measured for *trans*-**2** and **6** (Figure 2b). While strong emission was detected for the separated pyrene derivative in DMSO with a rather high fluorescence quantum yield ($\Phi_{fl,\mathbf{6}}$ = 0.30), a ~ 43-fold decrease was observed after incorporation into the ligand ($\Phi_{fl,trans\text{-}\mathbf{2}}$ = 0.007). A small fraction of this reduction must be attributed to the competitive absorption of the pyrene and azobenzene moieties of *trans*-**2** at the excitation wavelength of the fluorescence quantum yield measurements (λ_{exc}= 320 nm). Actually, according to the extinction coefficients measured for the reference compounds **6** and *trans*-**20** ($\varepsilon_{\mathbf{6}}^{320\,nm}/\varepsilon_{trans-\mathbf{20}}^{320\,nm} \sim 2$), about one third of the excitation photons in these experiments were absorbed by the non-emissive azoaromatic core of *trans*-**2**, thus accounting for an apparent ~ 1.5-fold decrease in Φ_{fl} for the pyrene antenna. However, the major part of the fluorescence quantum yield reduction (~ 30-fold) can be ascribed to an intrinsic decrement of the emission efficiency of this fluorophore upon tethering to the azobenzene group in *trans*-**2**, thus uncovering additional non-radiative relaxation pathways of its electronic excited state. As such, this result is indicative of the occurrence of the RET processes required for sensitization of the photoisomerization of the azobenzene moiety.

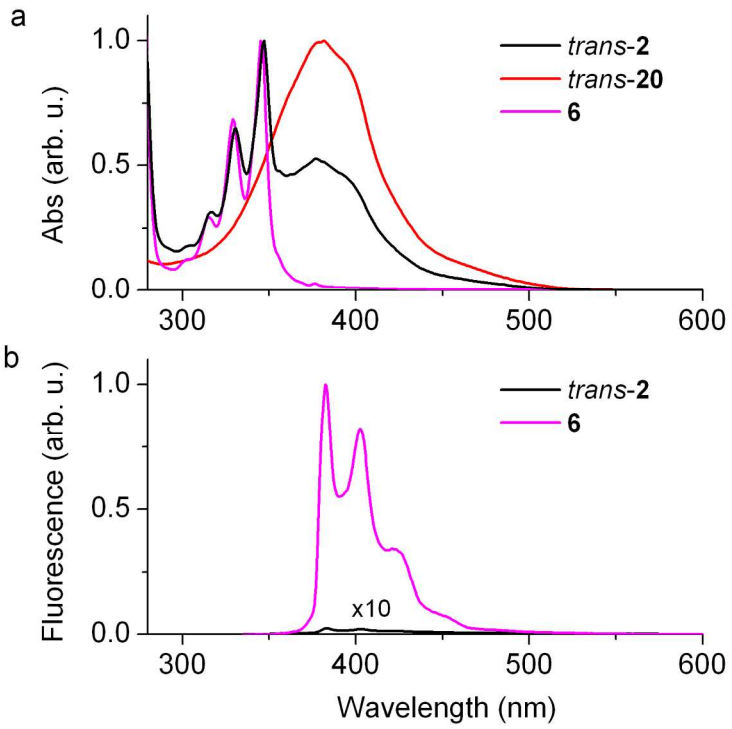

Figure 2. (a) Normalized absorption spectra of *trans*-**2**, **6** and *trans*-**20** in DMSO (c = 5 10^{-6} M). (b) Fluorescence emission spectra of *trans*-**2** (x10, λ_{exc} = 320 nm) and **6** (λ_{exc} = 305 nm) in DMSO (c = 1 10^{-6} M). Both emission spectra were normalized relative to the absorption at the excitation wavelength.

In spite of this, we first investigated *trans*-to-*cis* isomerization of **2** upon direct excitation of the azoaromatic moiety. Figure 3 depicts the changes registered in the absorption spectra of *trans*-**2** and reference compound *trans*-**20** in DMSO when irradiated at λ_{exc} = 365 nm, an excitation wavelength where the pyrene moiety of the ligand shows minimal absorption ($\varepsilon^{365\ nm}_{trans\text{-}\mathbf{20}}/\varepsilon^{365\ nm}_{\mathbf{6}}$ = 13; see Figure 2a). In both cases, a noteworthy decrease of the broad $\pi \rightarrow \pi^*$ azobenzene band around 380 nm and a very slight increase of the $n \rightarrow \pi^*$ azobenzene band at λ_{abs} > 450 nm were observed. These are clear signatures of the photoinduced conversion of *trans*-**2** and *trans*-**20** into their corresponding *cis* isomers,[4,7,16] which should lead to the formation of an equilibrium photostationary state (PSS). According to the ^{1}H NMR data measured for DMSO-d_6 solutions of these compounds under equivalent irradiation conditions, the *cis* composition of the PSS mixtures generated was found to be 65% and 63% for **2** and

20, respectively. Since nearly identical values were also determined for the *trans*-to-*cis* photoisomerization quantum yields of these azobenzene derivatives ($\Phi_{trans\text{-}cis,\mathbf{2}} = \Phi_{trans\text{-}cis,\mathbf{20}} = 0.28$), we could unambiguously conclude that the introduction of a pyrene group into the structure of ligand **2** did not modify the intrinsic photochemical behavior of its azoaromatic moiety when subjected to direct light excitation. A similar conclusion was drawn when analyzing the photoinduced *cis*-to-*trans* isomerization of **2** and **20** upon selective excitation of their azobenzene core. Thus, when illuminating with green light (λ_{exc} = 532 nm) the *trans*/*cis* mixtures of these compounds obtained by irradiation at λ_{exc} = 365 nm, our absorption measurements demonstrated that both *cis*-**2** and *cis*-**20** back-isomerized to their *trans* isomers nearly quantitatively and at similar rates (Figure S3). In particular, PSS mixtures with 94% and 93% content in *trans*-**2** and *trans*-**20** were obtained under these experimental conditions, respectively, according to our spectral data.

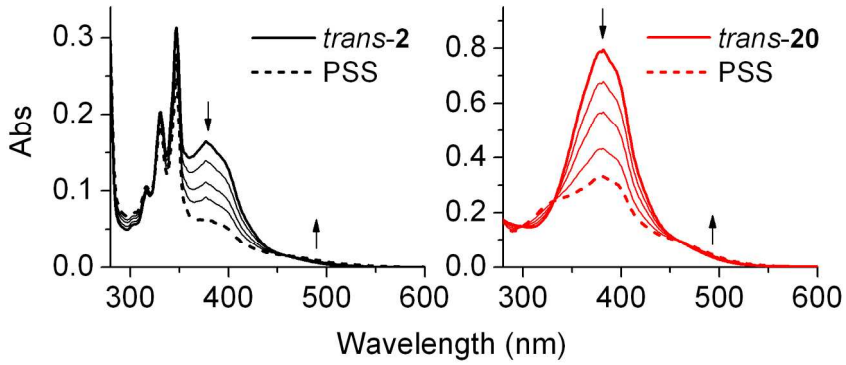

Figure 3. Variation of the absorption spectra of *trans*-**2** (c = 5 10^{-6} M) and *trans*-**20** (c = 2.7 10^{-5} M) in DMSO upon irradiation at λ_{exc} = 365 nm. The arrows in the figures indicate the spectral changes observed, while the dashed lines correspond to the absorption spectra of the resulting photostationary state mixtures.

Next, the photosensitized isomerization of *trans*-**2** upon irradiation of the pyrene antenna was explored. Unfortunately, selective excitation of this chromophore to prevent direct *trans*-to-*cis* isomerization of **2** could not be achieved because the absorption spectrum of the pyrene photosensitizer

selected fully overlaps with that of the azobenzene core (see Figure 2a). To minimize this effect and evaluate the actual contribution of the sensitized pathway to the photoswitching of **2**, two main actions were taken. On the one hand, photosensitization was investigated at λ_{exc} = 347 nm, for which the largest difference in absorption between the pyrene and azoaromatic fragments of *trans*-**2** was determined ($\varepsilon_{\mathbf{6}}^{347\ nm}/\varepsilon_{trans\text{-}\mathbf{20}}^{347\ nm}$ = 2). On the other hand, photoisomerization was simultaneously studied at λ_{exc} = 365 nm, which should selectively promote direct light-induced *trans*-to-*cis* conversion, as discussed above. Figure 4 shows the relative photoisomerization efficiencies of *trans*-**2** and antenna-less compound *trans*-**20** in DMSO solution at λ_{exc} = 347 and 365 nm, which are plotted as the photogenerated ratios of *cis*-**2** and *cis*-**20** determined at different irradiation times from absorption measurements. Noticeably, a straight line around $\%_{cis\text{-}\mathbf{2}} / \%_{cis\text{-}\mathbf{20}}$ =1 was obtained at λ_{exc} = 365 nm, which indicates that direct *trans*-to-*cis* photoisomerization proceeds with equivalent rates and efficiencies for both azoaromatic compounds. This is indeed the result expected according to our previous experiments, where nearly identical PSS compositions and $\Phi_{trans\text{-}cis}$ values were measured upon selective excitation of the *trans*-azobenzene moiety of **2** and **20**.

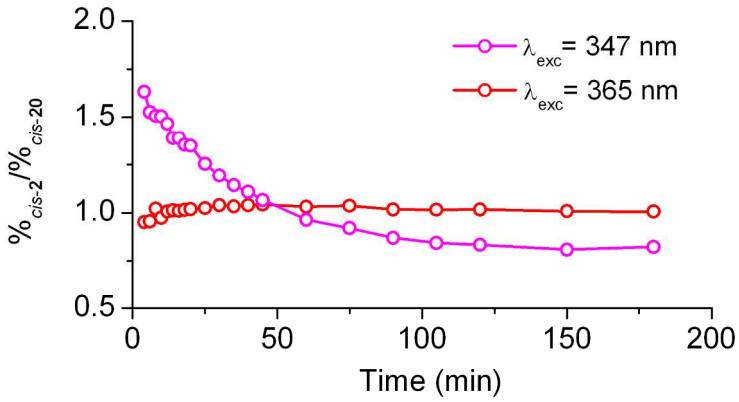

Figure 4. Photogenerated ratios of *cis*-**2** and *cis*-**20** ($\%_{cis\text{-}\mathbf{2}} / \%_{cis\text{-}\mathbf{20}}$) measured upon continuous irradiation of DMSO solutions of *trans*-**2** and *trans*-**20** (c = 5 10^{-6} M) at λ_{exc} = 347 and 365 nm.

However, a more complex time profile was obtained at λ_{exc} = 347 nm. At short irradiation times (t < 50 min), we found $\%_{cis\text{-}\mathbf{2}} / \%_{cis\text{-}\mathbf{20}}$ to be larger than 1, which indicates that *trans*-to-*cis* photoisomerization

takes place faster for ligand **2**. This pinpoints the occurrence of an additional light-induced isomerization mechanism in this compound with respect to reference *trans*-**20**, which we ascribe to photosensitization evolving through pyrene absorption and subsequent resonance energy transfer toward the azobenzene core. Such RET process would therefore account for the fluorescence quenching observed for the pyrene unit in the ligand (see Figure 2b) and, actually, we estimated it to take place with high critical Förster radius (R_0= 3.42 nm) and efficiency (E_{RET}= 99.8%) according to the optical properties of **6** and *trans*-**20** and the separation distances between the antenna and azoaromatic groups in *trans*-**2** (Figure S1). Nevertheless, it must be noted that energy transfer from pyrene to the *cis*-azobenzene moiety of **2** is also to be expected given the non-negligible spectral overlap between these groups and, indeed, only slightly lower R_0 and E_{RET} values were determined for this process with respect to that in *trans*-**2**: R_0= 2.47 nm and E_{RET}= 96.2% (Figure S2). This suggests that the *cis*-to-*trans* isomerization of this compound can also be photosensitized by the antenna once the concentration of *cis*-**2** significantly increases in the sample. As such, the PSS generated at λ_{exc} = 347 nm would depend on the intricate balance between direct and sensitized *trans*-to-*cis* and *cis*-to-*trans* photoisomerization rates, which explains the different equilibrium mixtures obtained under long irradiation times at this wavelength with respect to λ_{exc} = 365 nm. In spite of this, it is clear that addition of the pyrene group to the ligand enhances the photoconversion efficiency of *trans*-**2** (up to 60% according to the data at short irradiation times), thus demonstrating that photosensitization with a two-photon absorber can also be exploited to trigger MAGA-type PTLs bearing a symmetrically-substituted azobenzene core.

Once proven that target photoswitch **2** can operate under photosensitized isomerization, the thermal stability of the resulting *cis* isomer was analyzed. With this aim, the spontaneous *cis*-to-trans isomerization of this compound and reference **20** was studied in the dark and at room temperature by absorption spectroscopy. Spectral changes were observed in this way that are consistent with *cis*-**2** and *cis*-**20** back-isomerization -- namely, the recovery of the intense *trans* absorption around 380 nm and a slight decrease of the n $\rightarrow$ π^* band at λ_{abs} > 450 nm (Figure S4). By plotting the time dependence of this

data, the thermal *cis*-to-*trans* conversion rates could be retrieved from monoexponential fits,[17] as shown in Figure 5. In particular, the following values were obtained: $k_{cis\text{-}trans}$ = 3.2 10^{-5} and 4.1 10^{-5} s^{-1} for **2** and **20**, respectively, which correspond to thermal lifetimes of their *cis* isomers at room temperature of 8.7 h and 6.8 h. Clearly, very similar *cis*-to-*trans* isomerization kinetics were found for both compounds in the dark. This indicates that, under equivalent experimental conditions, the thermal stability of *cis*-azobenzenes is mainly governed by the electronic effects imparted by the substituents introduced, as already reported.[4] As such, the equivalent 4,4'-diamide substituent pattern of **2** and **20** accounts for their comparable and long τ_{cis} values regardless of the different nature of their actual substituents. In spite of this, a minor though non-negligible size effect could be inferred from our measurements, the bulkier amide groups introduced in **2** slightly slowing down its thermal *cis*-to-*trans* back-isomerization process and leading to a little larger *cis* state lifetime. On the other hand, the large thermal stability encountered for *cis*-**2** and *cis*-**20** is in agreement with the behavior previously reported for *cis*-MAG (τ_{cis}= 17.7 min in aqueous buffer)[7b], which also bears a 4,4'-diamidoazobenzene core. The differences in τ_{cis} observed between these compounds must be attributed to the distinct media where the measurements were conducted, since it is known that the *cis* lifetime of azobenzene derivatives largely decreases in polar solvents.[4a,25] In fact, when monitoring the thermal *cis*-to-*trans* isomerization kinetics of *cis*-**2** in a 1:1 DMSO:water mixture (Figure S5), we determined a much shorter τ_{cis} value (τ_{cis}= 2.0 h) than in pure DMSO and closer to that found for *cis*-MAG in aqueous buffer. Finally, the large thermal *cis* state stability obtained herein for **2** is in striking contrast with the short *cis* lifetime measured for the previous MAGA ligand **1** (τ_{cis}= 67 ms in PBS:DMSO 4:1 and 265 ms when tethered to LiGluR[16]), which arose from its push-pull substitution pattern. This unequivocally demonstrates that our photosensitized approach toward two-photon responsive azobenzene-based PTLs also enables the use of switches displaying long-lived *cis* isomers and, consequently, can be applied to the generation of large light-induced biological responses upon continuous irradiation.

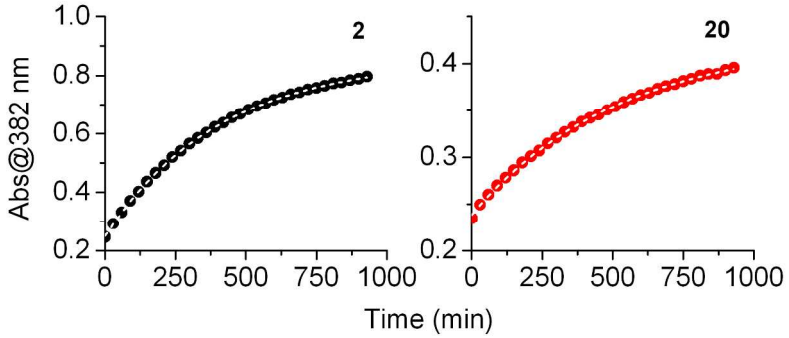

Figure 5. Variation of the absorption at 382 nm of the photostationary state mixtures of **2** and **20** in the dark at 25 ºC in DMSO, which reports on the recovery of the concentration of *trans*-**2** and *trans*-**20** upon thermal *cis*-to-*trans* isomerization. Points correspond to the experimental data, while dashed lines were obtained from monoexponential fits.

Actually, a preliminary assessment of the two-photon activity of **2** can be made on the basis of the one-photon experiments conducted herein, the two-photon absorption cross-sections reported in the literature for pyrene[26] and azobenzene[17] chromophores and our previous work on fast relaxing MAGA switch **1**.[16] Since the same excited state of the pyrene antenna would be built, the efficiency of the RET process towards the azobenzene core of **2** should be the same under one- or two-photon excitation. As such, the photosensitized two-photon response of this switch would mainly depend on the following parameters: (a) the selectivity of the two-photon excitation of the pyrene antenna with NIR light; (b) the lifetime of the *cis* isomer of the switch created under such conditions. As discussed above, the one-photon excitation of the pyrene moiety of **2** is poorly selective and the maximum photosensitization effect was found at λ_{exc} = 347 nm, where a 2:1 pyrene:azobenzene absorption ratio was estimated. Noticeably, we expect this absorption difference to increase under NIR irradiation due to the larger two-photon activity of the pyrene antenna, thus favoring the sensitized pathway for photoisomerization. In fact, 5-fold higher two-photon absorption cross-sections at 820 nm have been reported for monosubstituted pyrene derivatives (σ_2=55 GM; 1 GM= 10^{-50} cm^4 s γ^{-1}) with respect to 4,4'-diamidoazobenzenes (σ_2=10 GM).[17] As a result, sensitization via the pyrene antenna should be the

major pathway for the two-photon isomerization of **2**. It must be noted that the intrinsic efficiency of this process should be lower than for our previous MAGA switch **1** bearing a higher absorbing naphthalene sensitizer (σ_2~200 GM at 780 nm).[16,27] In spite of this, an overall large two-photon response would be expected for **2** on account of the longer lifetime of its *cis* isomer. Actually, the fast thermal back-isomerization of **1** resulted in a ~10-fold lower biological signal for this compound with respect to MAG under continuous one-photon excitation,[16] which indicated that a less *cis*-enriched photostationary state could be prepared for this MAGA switch. Taking into account that **2** also presents a long-lived *cis* state as MAG, a similar factor can be assumed between the one-photon responses of the two MAGA-type compounds. This should counterbalance the ~4-fold lower two-photon absorptivity of the pyrene sensitizer with respect to the naphthalene antenna of **1** and eventually lead to larger biological signals for the switch developed herein under NIR irradiation.

Conclusions

In summary, we report herein the synthesis and photochemical characterization of a new azobenzene-based photoswitchable ligand designed to enable optical control of ionotropic glutamate receptors in neurons via two-photon excitation of a pyrene sensitizing unit with NIR light. Aiming to develop an efficient and versatile synthetic route for this and other related ligands, a modular strategy is described which benefits from the use of a new linear full protected glutamate derivative stable in basic media. In this way, target compound **2** could be prepared in 7 steps with 27% overall yield starting from a commercial *N*,*N*-orthogonally diprotected L-lysine derivative as central scaffold, to which its different functional fragments were sequentially introduced: the azoaromatic switch, the glutamate moiety, the pyrene sensitizer and the anchoring maleimide group. As originally planned, **2** presents one-photon photoisomerization either upon selective irradiation of its azobenzene core, or via photoexcitation of the pyrene antenna. In addition, by using a symmetrically substituted azoaromatic group, the thermal lifetime of its *cis* isomer could be enhanced in a factor $>10^5$ with respect to the analogous two-photon

responsive ligands previously reported, which rely on the intrinsic non-linear optical properties of push-pull azobenzenes. This is an essential requirement for enabling accumulation of the protein-bound *cis* state of the switch upon repeated illumination of tagged glutamate receptors, which makes compound **2** a promising candidate for evoking large photoinduced biological responses under multiphoton operation of these systems with NIR light.

Experimental Section

General Methods: Commercially available reagents were used as received. The solvents were dried by distillation over the appropriate drying agents. All reactions were performed avoiding moisture by standard procedures and under nitrogen atmosphere. Flash column chromatography was performed using silica gel (230-400 mesh). ^{1}H NMR and ^{13}C NMR spectra were recorded at 250 and 62.5 MHz or 360 and 90 MHz or 500 and 125 MHz. NMR signals were assigned with the help of DEPT, COSY, HMBC, HMQC and NOESY experiments. Proton chemical shifts are reported in ppm (δ) ($CDCl_3$, δ 7.26; DMSO-d6, δ 2.50 or methanol-d_4, δ 3.31). Carbon chemical shifts are reported in ppm (δ) ($CDCl_3$, δ 77.2; DMSO-d6, δ 39.5 or methanol-d_4, δ 49.0). Melting points were determined on hot stage and are uncorrected. High resolution mass spectra (HRMS) were recorded in a micrOTOFQ spectrometer using ESIMS (QTOF). Optical rotations were measured at 22 ± 2 ˚C.

Photochemical characterization: All spectroscopic and photochemical experiments were carried out in HPLC or spectroscopy quality solvents and in Ar-degassed samples. Steady-state UV-vis absorption measurements were recorded on a UV-visible (190-1100 nm) Spectrophotometer. Fluorescence emission spectra were measured in a fluorescence spectrometer using high energy pulsed Xenon source for excitation. All the emission spectra registered were corrected by the wavelength dependence of the spectral response of the detection system. Fluorescence quantum yields were determined using the standard method[28] and relative to pyrene in ethanol (Φ_{pyrene} = 0.32).[29] The same excitation wavelength was used for both the sample of interest and the standard (λ_{exc} = 305 (**6**) or 320 nm (*trans*-**2**)) and

solutions with absorbance values below 0.05 were measured to prevent inner-filter effects. The fluorescence quantum yield of the target compound (Φ_{sample}) was determined by applying the following equation:[28]

$$\Phi_{sample} = \Phi_{ref} \frac{F_{sample}}{F_{ref}} \frac{Abs_{ref}}{Abs_{sample}} \frac{n^2_{sample}}{n^2_{ref}} \quad (1)$$

In this equation, Φ_{ref} is the fluorescence quantum yield of the standard, F_{sample} and F_{ref} are the integrated emission intensities measured for the sample and the standard, Abs_{sample} and Abs_{ref} are the optical densities of the sample and the standard at the excitation wavelength, and n_{sample} and n_{ref} are the refractive indices of the solvents used. Photoisomerization of **2** and **20** was investigated by: (i) steady-state UV-vis absorption spectroscopy for *trans*-to-*cis* and *cis*-to-*trans* photoisomerization and slow *cis*-to-*trans* thermal back-isomerization processes; (ii) ^{1}H NMR for the elucidation of the *trans*-to-*cis* photostationary state mixtures. Photoisomerization quantum yields were determined using the methodology reported in ref. 30 and azobenzene as reference compound ($\Phi_{trans\text{-}cis}$= 0.15 in acetonitrile[31]). Different excitation sources were used in the photochemical experiments depending on the spectral requirements: a UV lamp equipped with two 4W tubes emitting at 365 nm, a Xe lamp coupled to a spectrograph, the third harmonic of the Nd:YAG laser (λ_{exc} = 355 nm) or a cw laser diode at λ_{exc} = 532 nm (Z-Laser). All absorption, fluorescence and photochemical measurements of **2**, **6** and pyrene were carried at low enough concentrations as to prevent aggregation processes driven by π-stacking of pyrene units.

(2*R*)-2-{(2*S*)-3-(*tert*-Butoxy)-2-[(*tert*-butoxycarbonyl)amino]-3-oxopropyl}-4-pentenoic acid, 10. To an ice-cooled solution of **9a** (1.80 g, 5.53 mmol) in a mixture 5:2 of THF and water (75 mL), 1 M LiOH (8.0 mL, 8.00 mmol) was added. After stirring for 1 h at this temperature, the mixture was acidified to pH 2 with 1 M HCl and extracted with EtOAc (3x50 mL). The combined organic extracts were dried over anhydrous $MgSO_4$ and the solvent was removed under vacuum. The residue was purified by column chromatography (hexanes/EtOAc, 3:1) to furnish **10** (1.78 g, 5.18 mmol, 93% yield) as a

yellowish oil: $[\alpha]_D^{20}$ - 0.8 (*c* 1.47, CH_2Cl_2); ^{1}H NMR (360 MHz, $CDCl_3$) δ 5.74 (m, 1H, H-4), 5.39 (br d, $J_{NH,2^i}$ = 8.5 Hz, 1H, NH), 5.08 (m, 2H, H-5), 4.22 (m, 1H, H-2^i), 2.49 (m, 2H, H-2, H-3), 2.31-2.04 (m, 2H, H-3, H-1^i), 1.66 (m, 1H, H-1^i), 1.46 (s, 9H, $C(CH_3)_3$), 1.45 (s, 9H, $C(CH_3)_3$); ^{13}C NMR (90 MHz, $CDCl_3$) δ 178.6 (C-1), 171.3 (C-3^i), 156.3 (CO, carbamate), 134.8 (C-4), 117.8 (C-5), 82.7 ($C(CH_3)_3$), 80.7 ($C(CH_3)_3$), 52.7 (C-2^i), 41.8 (C-2), 36.4 (C-3), 35.2 (C-1^i), 28.4 ($C(CH_3)_3$), 28.1 ($C(CH_3)_3$); IR (ATR) 2978, 1707, 1367, 1247, 1150 cm^{-1}; HRMS (ESI+) calcd. for [$C_{17}H_{29}NO_6$+Na]: 366.1887; found: 366.1893.

Di(*tert*-butyl) (2*R*,4*S*)-2-allyl-4-[(*tert*-butoxycarbonyl)amino]pentanedioate, 11. To a solution of compound **10** (3.50 g, 7.28 mmol) in CH_2Cl_2 (90 mL), *tert*-butyl 2,2,2-trichloroacetimidate (2.6 mL, 14.6 mmol) and $BF_3{\cdot}OEt_2$ (370 μL, 2.96 mmol) were added. Then, a saturated aqueous solution of $NaHCO_3$ (20 mL) was added and the product was extracted with CH_2Cl_2 (3x50 mL). The combined organic extracts were dried over anhydrous $MgSO_4$ and the solvent was removed under vacuum. The resulting yellow oil was purified by column chromatography (hexanes/EtOAc, 3:1) to give **11** (1.64 g, 4.10 mmol, 56%) as a yellow solid: mp 86-89 °C (from hexanes/EtOAc); $[\alpha]_D^{20}$ + 10.7 (*c* 0.59, CH_2Cl_2); ^{1}H NMR (250 MHz, $CDCl_3$) δ 5.70 (ddt, $J_{2^i,3_{trans}{}^i}$ = 17.0 Hz, $J_{2^i,3_{cis}{}^i}$ = 10.1 Hz, $J_{2^i,1^i}$ = 6.8 Hz, 1H, H-2^i), 5.09 (m, 3H, 2xH-3^i, NH), 4.22 (m, 1H, H-4), 2.49-2.26 (m, 2H, H-1^i, H-2), 2.26-2.03 (m, 2H, H-1^i, H-3), 1.65 (m, 1H, H-3), 1.44 (m, 27H, 3x$C(CH_3)_3$); ^{13}C NMR (62.5 MHz, $CDCl_3$) δ 173.9/171.7 (C-1/C-5), 155.3 (CO, carbamate), 135.0 (C-2^i), 117.2 (C-3^i), 81.8 ($C(CH_3)_3$), 80.7 ($C(CH_3)_3$), 79.5 ($C(CH_3)_3$), 52.7 (C-4), 42.3 (C-2), 36.8 (C-1^i), 34.1 (C-3), 28.3 ($C(CH_3)_3$), 28.1 ($C(CH_3)_3$), 28.0 ($C(CH_3)_3$); IR (ATR) 3382, 2979, 1742, 1703, 1526, 1366, 1229, 1150 cm^{-1}; HRMS (ESI+) calcd. for [$C_{21}H_{37}NO_6$+Na]: 422.2513; found: 422.2520.

Di(*tert*-butyl) (2*S*,4*R*)-2-[(*tert*-butoxycarbonyl)amino]-4-[(2*E*)-4-oxo-2-butenyl]pentanedioate, 12. To a boiling solution of (4*R*)-**11** (2.30 g, 5.75 mmol) and crotonaldehyde (2.4 mL, 28.8 mmol) in dry CH_2Cl_2 (36 mL), Hoveyda-Grubbs II catalyst (56 mg, 89 μmol) was added in 3 portions. The mixture was heated to reflux for 2.5 h, when TLC analysis (hexanes/EtOAc, 2:1) showed no starting material.

The reaction mixture was filtered off through a pad of silica gel and concentrated. The crude was purified by column chromatography (hexanes/Et_2O, from 3:1 to 1:1) to provide **12** (2.19 g, 5.12 mmol, 89% yield) as a yellow oil: $[\alpha]_D^{20}$ + 88.4 (*c* 0.48, CH_2Cl_2); ^{1}H NMR (250 MHz, $CDCl_3$) δ 9.46 (d, $J_{CHO,3i}$ = 7.8 Hz, 1H, CHO), 6.73 (dt, $J_{2i,3i}$ = 15.7 Hz, $J_{2i,1i}$ = 6.7 Hz, 1H, H-2^i), 6.09 (dd, $J_{3i,2i}$ = 15.7 Hz, $J_{3i,CHO}$ = 7.8 Hz, 1H, H-3^i), 5.03 (d, $J_{NH,2}$ = 7.9 Hz, 1H, NH), 4.20 (m, 1H, H-2), 2.68-2.39 (m, 3H, H-4, 2xH-1^i), 2.15 (ddd, J_{gem} = 12.7 Hz, $J_{3,2}$ = 8.6 Hz, $J_{3,4}$ = 4.8 Hz, 1H, H-3), 1.64 (ddd, J_{gem} = 12.7 Hz, $J_{3,2}$ = 8.6 Hz, $J_{3,4}$ = 3.7 Hz, 1H, H-3), 1.44 (m, 27H, 3xC(CH_3)$_3$); ^{13}C NMR (90 MHz, $CDCl_3$) δ 193.6 (CHO), 173.1/171.4 (C-1/C-5), 155.3 (CO, carbamate), 154.4 (C-2^i), 134.7 (C-3^i), 82.4 (*C*(CH_3)$_3$), 81.7 (*C*(CH_3)$_3$), 79.9 (*C*(CH_3)$_3$), 52.5 (C-2), 41.6 (C-4), 35.4 (C-1^i), 34.8 (C-3), 28.4 (C(*C*H_3)$_3$), 28.2 (C(*C*H_3)$_3$), 28.1 (C(*C*H_3)$_3$); IR (ATR) 2977, 1699, 1392, 1367, 1251, 1150 cm^{-1}; HRMS (ESI+) calcd. for [$C_{22}H_{37}NO_7$+Na]: 450.2462; found: 450.2460.

(2*E*,5*R*,7*S*)-8-*tert*-Butoxy-5-(*tert*-butoxycarbonyl)-7-[(*tert*-butoxycarbonyl)amino]-8-oxo-2-octenoic acid, 13. To an ice-cooled solution of the aldehyde **12** (2.50 g, 5.85 mmol) in a 5:1 mixture of *t*-BuOH and water (240 mL), 2-methyl-2-butene (6.2 mL, 58.5 mmol), $NaH_2PO_4 \cdot 2H_2O$ (4.60 g, 29.2 mmol) and $NaClO_2$ (3.17 g, 35.1 mmol) were successively added. The resulting mixture was stirred at 0 °C for 1 h and warmed up to rt. The reaction mixture was stirred overnight. Then, water (30 mL) and a saturated aqueous solution of Na_2CO_3 were added until pH 8. The mixture was extracted with EtOAc (3x50 mL), dried over anhydrous $MgSO_4$ and concentrated under vacuum. Purification by column chromatography (hexanes/EtOAc/CH_3COOH, 4:1:0.1) gave **13** (2.00 g, 4.51 mmol, 77% yield) as a yellow oil: $[\alpha]_D^{20}$ + 59.8 (*c* 1.16, CH_2Cl_2); ^{1}H NMR (360 MHz, MeOH-d_4) δ 6.86 (dt, $J_{3,2}$ = 15.1 Hz, $J_{3,4}$ = 7.3 Hz, 1H, H-3), 5.84 (d, $J_{2,3}$ = 15.1 Hz, 1H, H-2), 4.06 (dd, $J_{7,6}$ = 10.6 Hz, $J_{7,6}$ = 3.8 Hz, 1H, H-7), 2.56 (m, 1H, H-5), 2.41 (m, 2H, H-4), 2.08 (m, 1H, H-6), 1.65 (m, 1H, H-6), 1.45 (m, 27H, 3xC(CH_3)$_3$); ^{13}C NMR (62.5 MHz, MeOH-d_4) δ 174.5/172.8/169.0 (C-1/C-8/CO, ester), 157.3 (CO, carbamate), 146.7 (C-3), 124.4 (C-2), 82.4 (*C*(CH_3)$_3$), 82.1 (*C*(CH_3)$_3$), 80.2 (*C*(CH_3)$_3$), 53.6 (C-7), 42.9 (C-5), 35.9 (C-4), 34.4 (C-6),

28.8 (C(CH_3)$_3$), 28.4 (C(CH_3)$_3$), 28.3 (C(CH_3)$_3$); IR (ATR) 2977, 2932, 1703, 1366, 1247, 1147 cm^{-1}; HRMS (ESI+) calcd. for [$C_{22}H_{37}NO_8$+Na]: 466.2411; found: 466.2417.

(5*R*,7*S*)-8-*tert*-Butoxy-5-(*tert*-butoxycarbonyl)-7-[(*tert*-butoxycarbonyl)amino]-8-oxooctanoic acid, 5. To a solution of olefine **13** (1.50 g, 3.38 mmol) in EtOAc (60 mL), 10% Pd/C (0.15 g) was added. The resulting suspension was stirred in a H_2 atmosphere for 16 h. Then, it was filtered through Celite® and the solvent was evaporated under vacuum. The resulting oil was purified by column chromatography (hexanes/EtOAc/CH_3COOH, 5:4:1) to afford a colourless oil identified as **5** (1.50 g, 3.36 mmol, quantitative yield): $[\alpha]_D^{20}$ + 66 (*c* 0.30, CH_2Cl_2); ^{1}H NMR (360 MHz, MeOH-d_4) δ 6.83 (d, $J_{NH,7}$ = 8.4 Hz, 1H, NH), 3.98 (m, 1H, H-7), 2.44 (m, 1H, H-5), 2.29 (td, $J_{2,3}$ = 6.8 Hz, $J_{2,4}$ = 3.7 Hz, 2H, H-2), 2.03 (m, 1H, H-6), 1.60 (m, 5H, 2xH-3, 2xH-4, H-6), 1.46 (m, 27H, 3xC(CH_3)$_3$); ^{13}C NMR (90 MHz, MeOH-d_4) δ 176.8/175.9/173.3 (C-1/C-8/CO, ester), 157.8 (CO, carbamate), 82.5 (*C*(CH_3)$_3$), 82.0 (*C*(CH_3)$_3$), 80.3 (*C*(CH_3)$_3$), 54.1 (C-7), 43.9 (C-5), 35.0 (C-6), 34.5 (C-2), 33.4 (C-4), 28.8 (C(CH_3)$_3$), 28.4 (C(CH_3)$_3$), 28.3 (C(CH_3)$_3$), 23.6 (C-1); IR (ATR) 2976, 1709, 1392, 1366, 1248, 1146 cm^{-1}; HRMS (ESI+) calcd. for [$C_{22}H_{39}NO_8$+Na]: 468.2568; found: 468.2570.

9*H*-Fluoren-9-ylmethyl *N*-[(5*S*)-6-{4-[(*E*)-2-(4-aminophenyl)-1-diazenyl]aniline}-5-[(*tert*-butoxycarbonyl)amino]-6-oxohexyl]carbamate, 14. To a stirred solution of 4-[(*E*)-(4-aminophenyl)-1-diazenyl]aniline (**4**) (1.00 g, 4.71 mmol) in dry THF (100 mL) under N_2 atmosphere, a solution of **3** (2.43 g, 5.19 mmol), EDCI (1.17 g, 6.10 mmol), HOBt (955 mg, 7.07 mmol), DIPEA (3.3 mL, 18.8 mmol) in dry THF (100 mL) was added. The reaction mixture was stirred overnight at rt. Then, the mixture was diluted with EtOAc (200 mL) and washed with water (2x100 mL). The organic layer was dried over anhydrous $MgSO_4$ and concentrated under vacuum. The residue was purified by column chromatography (from CH_2Cl_2 to CH_2Cl_2/EtOAc, 4:1) to deliver amide **14** (1.62 g, 2.45 mmol, 85% yield considering starting material consumed) as an orange solid and starting material (388 mg, 1.83 mmol): mp 94-97 ºC (from CH_2Cl_2/EtOAc); $[\alpha]_D^{20}$ - 9.70 (*c* 1.01, $CHCl_3$); ^{1}H NMR (250 MHz, $CDCl_3$) δ 8.73 (br s, 1H, C-1^{iii}NH), 7.77 (m, 6H, H-4, H-5, H-3^{iii}, H-5^{iii}, H-2^{iv}, H-6^{iv}), 7.65 (d, $J_{2^{iii},3^{iii}}$ = $J_{6^{iii},5^{iii}}$ =

8.0 Hz, 2H, H-2^{iii}, H-6^{iii}), 7.58 (d, $J_{1,2} = J_{8,7} = 7.2$ Hz, 2H, H-1, H-8), 7.38 (t, $J_{3,2} = J_{3,4} = J_{6,7} = J_{6,5} = 7.2$ Hz, 2H, H-3, H-6), 7.29 (td, $J_{2,3} = J_{2,1} = J_{7,8} = J_{7,6} = 7.2$ Hz, $J_{2,4} = J_{7,5} = 1.2$ Hz, 2H, H-2, H-7), 6.71 (d, $J_{3^{iv},2^{iv}} = J_{5^{iv},6^{iv}} = 8.8$ Hz, 2H, H-3^{iv}, H-5^{iv}), 5.34 (d, $J_{C\text{-}5^{ii}NH,5^{ii}} = 7.5$ Hz, 1H, C-5^{ii}NH), 4.95 (t, $J_{C\text{-}1^{ii}NH,1^{ii}} = 6.0$ Hz, 1H, C-1^{ii}NH), 4.41 (d, $J_{1^i,9} = 6.9$ Hz, 2H, H-1^{i}), 4.20 (m, 2H, H-5^{ii}, H-9), 4.06 (br s, 2H, NH_2), 3.19 (m, 2H, H-1^{ii}), 1.95 (m, 1H, H-4^{ii}), 1.72 (m, 1H, H-4^{ii}), 1.62-1.36 (m, 13H, 2xH-2^{ii}, 2xH-3^{ii}, $C(CH_3)_3$); ^{13}C NMR (100.6 MHz, $CDCl_3$) δ 170.8 (C-6^{ii}), 156.9 (CO, carbamate), 156.5 (CO, carbamate), 149.5 (C-4^{iii}, C-4^{iv}), 145.7 (C-1^{iv}), 144.0 (C-9a, C-8a), 141.4 (C-4a, C-4b), 139.4 (C-1^{iii}), 127.8 (C-3, C-6), 127.2 (C-2, C-7), 125.1 (C-1, C-8, C-2^{iv}, C-6^{iv}), 123.4 (C-3^{iii}, C-5^{iii}), 120.1 (C-4, C-6, C-2^{iii}, C-6^{iii}), 114.8 (C-3^{iv}, C-5^{iv}), 80.7 ($C(CH_3)_3$), 66.7 (C-1^{i}), 55.2 (C-5^{ii}), 47.4 (C-9), 40.3 (C-1^{ii}), 31.4 (C-4^{ii}), 29.5 (C-2^{ii}), 28.4 ($C(CH_3)_3$), 22.7 (C-3^{ii}); IR (ATR) 3323, 2926, 2856, 1687, 1665, 1596, 1504, 1245 cm^{-1}; HRMS (ESI+) calcd. for [$C_{38}H_{42}N_6O_5$+Na]: 685.3109; found: 685.3112.

9*H*-Fluoren-9-ylmethyl *N*-((5*S*)-5-amino-6-{4-[(*E*)-2-(4-aminophenyl)-1-diazenyl]anilino}-6-oxohexyl)carbamate, 15. To a solution of intermediate **14** (1.07 g, 1.62 mmol) in MeOH (100 mL), 37% HCl (21 mL, 0.22 mol) was added. The reaction mixture was stirred for 1 h at room temperature until TLC (EtOAc) showed no presence of starting material. Then, the mixture was concentrated under vacuum, diluted with EtOAc (20 mL) and neutralized with a saturated aqueous solution of $NaHCO_3$. Purification by column chromatography (from EtOAc to EtOAc/MeOH, 95:5) gave **15** (890 mg, 1.58 mmol, 98% yield) as an orange solid: mp 78-82 ºC (from EtOAc); $[\alpha]_D^{20}$ -25.6 (*c* 1.19, $CHCl_3$); ^{1}H NMR (400 MHz, $CDCl_3$) δ 9.69 (br s, 1H, C-1^{iii}NH), 7.84 (d, $J_{3^{iii},2^{iii}} = J_{5^{iii},6^{iii}} = 8.7$ Hz, 2H, H-3^{iii}, H-5^{iii}), 7.75 (m, 6H, H-4, H-5, H-2^{iii}, H-6^{iii}, H-2^{iv}, H-5^{iv}), 7.59 (d, $J_{1,2} = J_{8,7} = 7.4$ Hz, 2H, H-1, H-8), 7.39 (t, $J_{3,2} = J_{3,4} = J_{6,7} = J_{6,5} = 7.4$ Hz, 2H, H-3, H-6), 7.31 (td, $J_{2,3} = J_{2,1} = J_{7,8} = J_{7,6} = 7.4$ Hz, $J_{2,4} = J_{7,5} = 0.9$ Hz, 2H, H-2, H-7), 6.73 (d, $J_{3^{iv},2^{iv}} = J_{5^{iv},6^{iv}} = 8.7$ Hz, 2H, H-3^{iv}, H-5^{iv}), 4.90 (t, $J_{C\text{-}1^{ii}NH,1^{ii}} = 5.4$ Hz, 1H, C-1^{ii}NH), 4.40 (d, $J_{1^i,9} = 6.9$ Hz, 2H, H-1^{i}), 4.21 (t, $J_{9,1^i} = 6.5$ Hz, 1H, H-9), 3.49 (m, 1H, H-5^{ii}), 3.21 (m, 2H, H-1^{ii}), 1.96 (m, 1H, H-4^{ii}), 1.68-1.29 (m, 5H, 2xH-2^{ii}, 2xH-3^{ii}, H-4^{ii}); ^{13}C NMR (100.6 MHz, $CDCl_3$) δ 173.5 (C-6^{ii}), 156.7 (CO, carbamate), 149.5/149.4 (C-4^{iii}/C-4^{iv}), 145.7 (C-1^{iv}), 144.1 (C-9a, C-

8a), 141.4 (C-4a, C-4b), 139.4 (C-1^{iii}), 127.8 (C-3, C-6), 127.2 (C-2, C-7), 125.1 (C-1, C-8, C-2^{iv}, C-6^{iv}), 123.5 (C-3^{iii}, C-5^{iii}), 120.1 (C-4, C-6), 119.6 (C-2^{iii}, C-6^{iii}), 114.8 (C-3^{iv}, C-5^{iv}), 66.7 (C-1^{i}), 55.5 (C-5^{ii}), 47.4 (C-9), 40.7 (C-1^{ii}), 34.5 (C-4^{ii}), 29.8 (C-2^{ii}), 23.0 (C-3^{ii}); IR (ATR) 3335, 2923, 1687, 1596, 1508, 1249, 1138 cm^{-1}; HRMS (ESI+) calcd. for $[C_{33}H_{34}N_6O_3+H]$: 563.2765; found: 563.2769.

Di(*tert*-butyl) (2*R*,4*S*)-2-{4-[((1*S*)-1-{4-[(*E*)-(4-aminophenyl)-1-diazenyl]anilino} carbonyl-5-{[(9*H*-fluoren-9-ylmethoxy)carbonyl]amino}pentyl)amino]-4-oxobutyl}-4-[(*tert*-butoxycarbonyl)amino]pentanedioate, 16. To a stirred solution of **15** (232 mg, 0.34 mmol) in dry THF (18 mL) under N_2 atmosphere, a solution of **5** (169 mg, 0.38 mmol), EDCI (86 mg, 0.45 mmol), HOBt (70 mg, 0.52 mmol), DIPEA (240 μL, 1.40 mmol) in dry THF (20 mL) was added. The reaction mixture was stirred overnight at rt. Then, the mixture was diluted with EtOAc (40 mL) and washed with water (2x40 mL). The organic layer was dried over anhydrous $MgSO_4$ and concentrated under vacuum. The residue was purified by column chromatography (hexanes/EtOAc, 1:9) to afford amide **16** (335 mg, 0.30 mmol, 88% yield) as an orange solid: mp 98-105 °C (from hexanes/EtOAc); $[\alpha]_D^{20}$ - 22.5 (*c* 1.18, $CHCl_3$); ^1H NMR (400 MHz, $CDCl_3$) δ 8.91 (br s, 1H, C-1^{v}NH), 7.79 (m, 6H, H-4^{iv}, H-5^{iv}, H-3^{v}, H-5^{v}, H-2^{vi}, H-6^{vi}), 7.65 (d, $J_{2v,3v} = J_{6v,5v}$ = 8.7 Hz, 2H, H-2^{v}, H-6^{v}), 7.57 (d, $J_{1iv,2iv} = J_{8i,7iv}$ = 7.4 Hz, 2H, H-1^{iv}, H-8^{iv}), 7.38 (t, $J_{3iv,2iv} = J_{3iv,4iv} = J_{6iv,5iv} = J_{6iv,7iv}$ = 7.4 Hz, 2H, H-3^{iv}, H-6^{iv}), 7.31 (t, $J_{2iv,3iv} = J_{2iv,1iv} = J_{7iv,6iv} = J_{7iv,8i}$ = 7.4 Hz, 2H, H-2^{iv}, H-7^{iv}), 6.73 (d, $J_{3vi,2vi} = J_{5vi,6vi}$ = 8.7 Hz, 2H, H-3^{vi}, H-5^{vi}), 6.48 (s, 1H, C-1^{ii}NH), 5.10 (t, $J_{C\text{-}5^{ii}NH,5^{ii}}$ = 5.4 Hz, 1H, C-5^{ii}NH), 4.56 (m, 1H, H-1^{ii}), 4.38 (d, $J_{1iii,9iv}$ = 6.9 Hz, 2H, H-1^{iii}), 4.20 (m, 2H, H-4, H-9^{iv}), 4.05 (br s, 2H, NH_2), 3.22 (m, 2H, H-5^{ii}), 2.34 (m, 1H, H-2), 2.24 (m, 2H, H-3^{i}), 2.13-1.94 (m, 3H, H-3, H-1^{i}, H-2^{ii}), 1.86-1.37 (m, 7H, H-3, H-1^{i}, 2xH-2^{i}, H-2^{ii}, 2xH-4^{ii}), 1.44 (m, 29H, 3x$C(CH_3)_3$, 2xH-3^{ii}); ^{13}C NMR (100.6 MHz, $CDCl_3$) δ 174.5/173.8/171.9/170.1 (C-1/C-5/C-4^{i}/CO, amide), 157.0 (CO, carbamate), 155.5 (CO, carbamate), 149.5 (C-4^{v}/C-4^{vi}), 145.7 (C-1^{vi}), 144.1 (C-$9a^{iv}$, C-$8a^{iv}$), 141.4 (C-$4a^{iv}$, C-$4b^{iv}$), 139.5 (C-1^{v}), 127.8 (C-3^{iv}, C-6^{iv}), 127.2 (C-2^{iv}, C-7^{iv}), 125.2/125.1 (C-1^{iv}, C-8^{iv}/C-2^{vi}, C-6^{vi}), 123.4 (C-3^{v}, C-5^{v}), 120.1 (C-4^{iv}, C-5^{iv}/C-2^{v}, C-6^{v}), 114.8 (C-3^{vi}, C-5^{vi}), 82.1 ($C(CH_3)_3$), 81.1 ($C(CH_3)_3$), 79.8 ($C(CH_3)_3$), 66.8 (C-1^{iii}), 54.0 (C-1^{ii}), 52.8 (C-4), 47.4 (C-

9^{iv}), 42.4 (C-2), 40.5 (C-5^{ii}), 36.1 (C-3^{i}), 34.9 (C-3), 32.1 (C-1^{i}), 30.7 (C-2^{ii}), 29.8 (C-4^{ii}), 28.5 (C(CH_3)$_3$), 28.2 (C(CH_3)$_3$), 28.1 (C(CH_3)$_3$), 23.2 (C-2^{i}), 22.6 (C-3^{ii}); IR (ATR) 3300, 2976, 2931, 1691, 1598, 1530, 1366, 1248, 1148 cm^{-1}; HRMS (ESI+) calcd. for [$C_{55}H_{71}N_7O_{10}$+H]: 990.5335; found: 990.5347.

Di(*tert*-butyl) (2*R*,4*S*)-2-(4-{(1*S*)-5-amino-1-({4-[(*E*)-(4-aminophenyl)-1-diazenyl] anilino}carbonyl) pentyl]amino}-4-oxobutyl)-4-[(*tert*-butoxycarbonyl)amino]pentanedioate, 17. A commercially available solution of 20% piperidine in DMF (18 mL) was added to compound **16** (775 mg, 0.78 mmol). After 1 h of stirring at rt, TLC analysis (EtOAc/MeOH, 95:5) showed no presence of starting material. The mixture was diluted with water (18 mL) and washed with EtOAc (3x30 mL). The combined organic extracts were dried over anhydrous $MgSO_4$ and concentrated under vacuum. The resulting solid was purified by column chromatography (from EtOAc to EtOAc/MeOH/NH_3, 9:2:1) to deliver **17** (459 mg, 0.60 mmol, 76% yield) as an orange solid: mp 89-96 °C (from EtOAc); $[\alpha]_D^{20}$ - 31.1 (*c* 0.88, $CHCl_3$); ^{1}H NMR (400 MHz, $CDCl_3$) δ 9.56 (br s, 1H, C-1^{iii}NH), 7.81 (m, 4H, H-3^{iii}, H-5^{iii}, H-2^{iv}, H-6^{iv}), 7.70 (d, $J_{2iii,3iii} = J_{6iii,5iii}$ = 7.7 Hz, 2H, H-2^{iii}, H-6^{iii}), 6.74 (d, $J_{3iv,2iv} = J_{5iv,6iv}$ = 8.4 Hz, 2H, H-3^{iv}, H-5^{iv}), 6.68 (m, 1H, C-1^{ii}NH), 5.21 (m, 1H, C-4NH), 4.63 (m, 1H, H-1^{ii}), 4.19 (m, 1H, H-4), 4.06 (br s, 2H, C-4^{iv}NH_2), 2.82 (m, 2H, H-5^{ii}), 2.58-2.31 (m, 3H, H-2, C-5^{ii}NH_2), 2.27 (m, 2H, H-3^{i}), 2.20-1.90 (m, 3H, H-3, H-1^{i}, H-2^{ii}), 1.86-1.56 (m, 7H, H-3, H-1^{i}, 2xH-2^{i}, H-2^{ii}, 2xH-4^{ii}), 1.44 (m, 29H, 3xC(CH_3)$_3$, 2xH-3^{ii}); ^{13}C NMR (100.6 MHz, $CDCl_3$) δ 174.5/173.5/171.8/170.3 (C-1/C-5/C-4^{i}/CO, amide), 155.4 (CO, carbamate), 149.5 (C-4^{iii}, C-4^{iv}), 145.7 (C-1^{iv}), 139.7 (C-1^{iii}), 125.1 (C-2^{iv}, C-6^{iv}), 123.4 (C-3^{iii}, C-5^{iii}), 120.1 (C-2^{iii}, C-6^{iii}), 114.8 (C-3^{iv}, C-5^{iv}), 82.7 (*C*(CH_3)$_3$), 81.1 (*C*(CH_3)$_3$), 79.7 (*C*(CH_3)$_3$), 53.9 (C-1^{ii}), 52.8 (C-4), 42.4 (C-2), 41.2 (C-5^{ii}), 36.1 (C-3^{i}), 34.8 (C-3), 32.1 (C-1^{i}/C-2^{ii}), 31.6 (C-4^{ii}), 28.5 (C(CH_3)$_3$), 28.2 (C(CH_3)$_3$), 28.1 (C(CH_3)$_3$), 23.2 (C-2^{i}), 22.7 (C-3^{ii}); IR (ATR) 3343, 2977, 2933, 1701, 1598, 1506, 1368, 1249, 1150 cm^{-1}; HRMS (ESI+) calcd. for [$C_{40}H_{61}N_7O_8$+H]: 768.4654; found: 768.4650.

Di(*tert*-butyl) (2*R*,4*S*)-2-(4-{(1*S*)-1-({4-[(*E*)-(4-aminophenyl)-1-diazenyl]anilino} carbonyl)-5-[(2-pyrenylacetyl)amino]pentyl}amino)-4-oxobutyl]-4-[(*tert*-butoxycarbonyl)amino]pentanedioate, 18.

To a stirred solution of **17** (410 mg, 0.53 mmol) in dry THF (20 mL) under N_2 atmosphere, a solution of 1-pyreneacetic acid (**6**) (167 mg, 0.64 mmol), EDCI (133 mg, 0.69 mmol), DIPEA (465 μL, 2.67 mmol) in dry THF (30 mL) was added. The reaction mixture was stirred overnight at rt. Then, the mixture was diluted with EtOAc (50 mL) and washed with water (2x20 mL). The organic layer was dried over anhydrous $MgSO_4$ and concentrated under vacuum. The residue was purified by column chromatography (EtOAc) and triturated with diethyl ether (2x10 mL) to furnish an orange solid identified as **18** (458 mg, 0.45 mmol, 84% yield): mp 157-161 °C (from EtOAc); $[\alpha]_D^{20}$ + 5.30 (*c* 0.96, $CHCl_3$); ^{1}H NMR (400 MHz, DMSO-d_6) δ 10.3 (s, 1H, C-1^{iv}NH), 8.37 (d, J = 9.3 Hz, 1H, H-pyr), 8.29-8.17 (m, 5H, C-1^{ii}NH, 4xH-pyr), 8.12 (s, 2H, H-pyr), 8.08 (m, 1H, C-5^{ii}NH), 8.05 (t, J = 7.6 Hz, 1H, H-pyr), 7.99 (d, J = 7.9 Hz, 1H, H-pyr), 7.76 (d, $J_{2^{iv},3^{iv}} = J_{5^{iv},6^{iv}}$ = 9.1 Hz, 2H, H-2^{iv}, H-6^{iv}), 7.71 (d, $J_{3^{iv},2^{iv}} = J_{5^{iv},6^{iv}}$ = 9.1 Hz, 2H, H-3^{iv}, H-5^{iv}), 7.63 (d, $J_{2^{v},3^{v}} = J_{6^{v},5^{v}}$ = 8.8 Hz, 2H, H-2^{v}, H-6^{v}), 7.10 (d, $J_{C\text{-}4NH,4}$ = 8.2 Hz, 1H, C-4NH), 6.66 (d, $J_{3^{v},2^{v}} = J_{5^{v},6^{v}}$ = 8.8 Hz, 2H, H-3^{v}, H-5^{v}), 6.02 (s, 2H, NH_2), 4.40 (m, 1H, H-1^{ii}), 4.17 (s, 2H, H-2^{iii}), 3.76 (m, 1H, H-4), 3.09 (dd, $J_{5^{ii},4^{ii}}$ = 12.6 Hz, $J_{5^{ii},C\text{-}5^{ii}NH}$ = 6.7 Hz, 2H, H-5^{ii}), 2.33 (m, 1H, H-2), 2.12 (m, 2H, H-3^{i}), 1.85-1.51 (m, 6H, 2xH-3, 2xH-1^{i}, 2xH-2^{ii}), 1.52-1.25 (m, 33H, 3xC(CH_3)$_3$, 2xH-2^{i}, 2xH-3^{ii}, 2xH-4^{ii}); ^{13}C NMR (100.6 MHz, DMSO-d_6) δ 173.8/172.1/171.7/171.2 (C-1/C-5/C-4^{i}/CO, amide), 169.9 (C-1^{iii}), 155.5 (CO, carbamate), 152.4 (C-4^{v}), 148.1 (C-4^{iv}), 142.8 (C-1^{v}), 140.2 (C-1^{iv}), 131.1 (C-pyr), 130.8 (C-pyr), 130.4 (C-pyr), 129.7 (C-pyr), 129.0 (C-pyr), 128.6 (CH-pyr), 127.4 (CH-pyr), 127.2 (CH-pyr), 126.8 (CH-pyr), 126.1 (CH-pyr), 125.1 (C-2^{v}, C-6^{v}), 124.9 (CH-pyr), 124.8 (CH-pyr), 124.7 (CH-pyr), 124.1 (C-pyr), 124.0 (CH-pyr), 123.9 (C-pyr), 122.5 (C-3^{iv}, C-5^{iv}), 119.5 (C-2^{iv}, C-6^{iv}), 113.4 (C-3^{v}, C-5^{v}), 80.3 (*C*(CH_3)$_3$), 79.7 (*C*(CH_3)$_3$), 78.0 (*C*(CH_3)$_3$), 53.4 (C-1^{ii}), 52.5 (C-4), 42.2 (C-2), 40.1 (C-1^{iii}), 38.6 (C-5^{ii}), 34.8 (C-3^{i}), 33.0 (C-3), 32.0 (C-1^{i}), 31.6 (C-2^{ii}), 28.8 (C-4^{ii}), 28.2 (C(*C*H_3)$_3$), 27.9 (C(*C*H_3)$_3$), 27.6 (C(*C*H_3)$_3$), 23.0 (C-3^{ii}, C-2^{i}); IR (ATR) 3277, 2975, 2935, 1720, 1638, 1599, 1531, 1506, 1368, 1251, 1151 cm^{-1}; HRMS (ESI+) calcd. for [$C_{58}H_{71}N_7O_9$+H]: 1010.5386; found: 1010.5377.

Di(*tert*-butyl) (2*S*,4*R*)-2-[(*tert*-butoxycarbonyl)amino]-4-[4-({(1*S*)-1-({4-[(*E*)-(4-{[2-(2,5-dioxo-2,5-dihydro-1*H*-1-pyrrolyl)-acetyl]amino}phenyl)-1-diazenyl]anilino}carbonyl)-5-[(2-pyrenylacetyl)amino]pentyl}amino)-4-oxobutyl]pentanedioate, 19. To a stirred solution of **7** (120 mg, 0.77 mmol) and oxalyl chloride 2.0 M in THF (402 μL, 0.80 mmol) in dry CH_2Cl_2 (12 mL) was added one drop of DMF. After stirring for 2 h at rt, the mixture was concentrated. The resulting acid chloride was taken up in dry THF (5 mL) and slowly added to an ice-cooled solution of **18** (200 mg, 0.20 mmol), DIPEA (207 μL, 1.19 mmol) in dry THF (25 mL). After stirring for 10 min at this temperature, the mixture was warmed up to rt and stirred for additional 4 h. Then, it was diluted with EtOAc (30 mL) and washed with water (3x10 mL). The organic extract was dried over anhydrous $MgSO_4$, concentrated under vacuum and purified by column chromatography (EtOAc/MeOH, 9:1) to provide **19** (168 mg, 0.15 mmol, 74% yield) as an orange solid: mp 187-198 °C (from EtOAc); $[\alpha]_D^{20}$ + 68.5 (*c* 0.70, DMSO); ^{1}H NMR (400 MHz, DMSO-d_6) δ 10.7 (s, 1H, C-4^{v}NH), 10.3 (s, 1H, C-1^{iv}NH), 8.37 (d, *J* = 9.3 Hz, 1H, H-pyr), 8.29-8.17 (m, 5H, C-1^{ii}NH, 4xH-pyr), 8.14 (s, 2H, H-pyr), 8.09 (m, 1H, C-5^{ii}NH), 8.07 (t, *J* = 7.8 Hz, 1H, H-pyr), 7.98 (d, *J* = 7.8 Hz, 1H, H-pyr), 7.84 (m, 6H, H-2^{iv}, H-6^{iv}, H-3^{iv}, H-5^{iv}, H-3^{v}, H-5^{v}), 7.75 (d, $J_{2v,3v} = J_{6v,5v}$ = 8.9 Hz, 2H, H-2^{v}, H-6^{v}), 7.16 (s, 2H, H-3^{vii}, H-4^{vii}), 7.09 (d, $J_{C\text{-}2NH,2}$ = 8.0 Hz, 1H, C-2NH), 4.38 (m, 1H, H-1^{ii}), 4.33 (s, 2H, H-2^{vi}), 4.16 (s, 2H, H-2^{iii}), 3.76 (m, 1H, H-2), 3.08 (dd, $J_{5ii,4ii}$ = 12.6 Hz, $J_{5ii,C\text{-}5iiNH}$ = 6.7 Hz, 2H, H-5^{ii}), 2.31 (m, 1H, H-4), 2.11 (m, 2H, H-3^{i}), 1.85-1.51 (m, 6H, 2xH-3, 2xH-1^{i}, 2xH-2^{ii}), 1.51-1.24 (m, 33H, 3xC(CH$_3$)$_3$, 2xH-2^{i}, 2xH-3^{ii}, 2xH-4^{ii}); ^{13}C NMR (100.6 MHz, DMSO-d_6) δ 172.8/171.1/170.7/170.5/169.7 (C-1/C-5/C-4^{i}/C-2^{vii}, C-5^{vii}/CO, amide), 168.9 (C-1^{iii}), 164.3 (C-1^{vi}), 154.5 (CO, carbamate), 146.9/146.7 (C-4^{iv}/C-1^{v}), 140.7/140.1 (C-1^{iv}/C-4^{v}), 134.0 (C-3^{vii}, C-4^{vii}), 130.1 (C-pyr), 129.8 (C-pyr), 129.4 (C-pyr), 128.7 (C-pyr), 128.0 (C-pyr), 127.6 (CH-pyr), 126.4 (CH-pyr), 126.2 (CH-pyr), 125.8 (CH-pyr), 125.1 (CH-pyr), 124.1 (CH-pyr), 123.9 (CH-pyr), 123.7 (CH-pyr), 123.1 (C-pyr), 123.0 (CH-pyr), 122.9 (C-pyr), 122.5/122.4 (C-2^{v}, C-6^{v}/C-3^{iv}, C-5^{iv}), 118.5 (C-2^{iv}, C-6^{iv}, C-3^{v}, C-5^{v}), 79.3 (*C*(CH$_3$)$_3$), 78.7 (*C*(CH$_3$)$_3$), 77.0 (*C*(CH$_3$)$_3$), 52.4 (C-1^{ii}), 51.6 (C-2), 41.2 (C-4), 39.5 (C-2^{iii}), 37.6 (C-5^{ii}), 33.8 (C-3^{i}), 32.0 (C-3), 31.0 (C-1^{i}), 30.6 (C-2^{ii}),

27.8 (C-4^{ii}), 27.2 (C(CH$_3$)$_3$), 26.9 (C(CH$_3$)$_3$), 26.6 (C(CH$_3$)$_3$), 22.0 (C-3^{ii}, C-2^{i}); IR (ATR) 3274, 2976, 2933, 1716, 1528, 1366, 1247, 1148 cm^{-1}; HRMS (ESI+) calcd. for [$C_{64}H_{74}N_8O_{12}$+Na]: 1169.5318; found: 1169.5350.

{(1*S*,3*R*)-1,3-Dicarboxy-7-[((1*S*)-1-({4-[(*E*)-2-(4-{[2-(2,5-dioxo-2,5-dihydro-1*H*-1-pyrrolyl)acetyl]amino}phenyl)-1-diazenyl]anilino}carbonyl)-5-{[2-(2-pyrenyl)acetyl]amino}pentyl)amino]-7-oxoheptyl}ammonium 2,2,2-trifluoroacetate, 2. To a stirred solution of compound **19** (40 mg, 45 μmol) in CH_2Cl_2 (7.0 mL), trifluoroacetic acid (3.5 mL, 45.4 mmol) was added. The mixture was stirred at room temperature until the starting material was consumed as judged by TLC analysis (EtOAc/MeOH, 9:1). Then, the mixture was concentrated under vacuum and the resulting purple solid was triturated with diethyl ether (2x8 mL) to furnish **2** (29 mg, 28 μmol, 79%) as a brown powder: $[\alpha]_D^{20}$ + 50.9 (*c* 0.43, DMSO); ^{1}H NMR (400 MHz, DMSO-d$_6$) δ 10.7 (s, 1H, C-4^{iv}NH), 10.4 (s, 1H, C-1^{iii}NH), 8.37 (d, J = 9.3 Hz, 2H, H-pyr, C-1^{i}NH), 8.30-8.17 (m, 5H, C-5^{i}NH, 4xH-pyr), 8.14 (s, 2H, H-pyr), 8.05 (t, J = 7.6 Hz, 1H, H-pyr), 7.98 (d, J = 7.6 Hz, 1H, H-pyr), 7.84 (m, 6H, H-2^{iii}, H-6^{iii}, H-3^{iii}, H-5^{iii}, H-3^{iv}, H-5^{iv}), 7.76 (d, $J_{2^{iv},3^{iv}} = J_{6^{iv},5^{iv}}$ = 8.6 Hz, 2H, H-2^{iv}, H-6^{iv}), 7.16 (s, 2H, H-3^{vi}, H-4^{vi}), 4.36 (m, 1H, H-1^{i}), 4.33 (s, 2H, H-2^{v}), 4.19 (s, 3H, 2xH-2^{ii}, H-1), 3.08 (m, 2H, H-5^{i}), 2.68 (m, 1H, H-3), 2.12 (m, 3H, H-2, 2xH-6), 1.80-1.26 (m, 11H, H-2, 2xH-4, 2xH-5, 2xH-4^{i}, 2xH-3^{i}, 2xH-2^{i}); ^{13}C NMR (100.6 MHz, DMSO-d$_6$) δ 175.9/172.3/171.7/170.7/170.0 (C-2^{vi}/C-7/C-1^{ii}/CO, acid/CO, acid/CO, amide), 165.4 (C-1^{v}), 147.9/147.6 (C-4^{iii}/C-1^{iv}), 141.8/141.1 (C-1^{iii}/C-4^{iv}), 135.0 (C-3^{vi}, C-4^{vi}), 131.1 (C-pyr), 130.8 (C-pyr), 130.4 (C-pyr), 129.7 (C-pyr), 129.0 (C-pyr), 128.6 (CH-pyr), 127.4 (CH-pyr), 127.2 (CH-pyr), 126.8 (CH-pyr), 126.1 (CH-pyr), 125.1 (CH-pyr), 124.9 (CH-pyr), 124.7 (CH-pyr), 124.1 (2xC-pyr), 123.9 (C-pyr), 123.4 (C-2^{iv}, C-6^{iv}, C-3^{iii}, C-5^{iii}), 119.5 (C-2^{iii}, C-6^{iii}, C-3^{iv}, C-5^{iv}), 53.8 (C-1^{i}), 51.6 (C-1), 40.4 (C-3), 39.5 (C-2^{ii}), 38.5 (C-5^{i}), 36.6 (C-6), 32.3 (C-2), 31.4 (C-4), 30.8 (C-2^{i}), 28.8 (C-4^{i}), 23.0/22.7 (C-3^{i}, C-5); IR (ATR) 3277, 3044, 2938, 1712, 1644, 1595, 1532, 1199, 1150 cm^{-1}; HRMS (ESI+) calcd. for [$C_{51}H_{50}N_8O_{10}$+H]: 935.3723; found: 935.3714.

Acknowledgments. We acknowledge financial support from Ministerio de Economia y Competitividad (MINECO) (projects CTQ2012-30853 and CTQ2013-41161-R) and M.G.-M. thanks the "Universitat Autònoma de Barcelona" for a pre-doctoral grant. We also acknowledge financial support from the RecerCaixa foundation (2010ACUP00378); the Marató de TV3 Foundation (grant 111531); the European Union's Seventh Framework Programme for research, technological development and demonstration under grant agreements 270483, 210355 and 335011; the Catalan government (2012FI_B 01122 and 2014SGR-1251); the Spanish Government (CTQ2013-43892R); the Ramón Areces foundation and the ERANET SynBio program.

Supporting Information Available: Additional photochemical data, ^{1}H and ^{13}C NMR spectra of all new compounds and HSQC spectrum for compounds **10**, **16** and **18**. This material is available free of charge via the Internet at http://pubs.acs.org.

References

[1] (a) Fenno, L.; Yizhar, O.; Deisseroth, K. *Annu. Rev. Neurosci*. **2011**, *34*, 389-412. (b) Deisseroth, K. *Nat. Methods* **2011**, *8*, 26-29.

[2] Fehrentz, T.; Schönberger, M.; Trauner, D. *Angew. Chem. Int. Ed*. **2011**, *50*, 12156-12182.

[3] Kramer, R. H. ; Mourot, A.; Adesnik, H. *Nat. Neurosci*. **2013**, *16*, 816-823.

[4] (a) Beharry, A. A.; Woolley, G. A. *Chem. Soc. Rev.* **2011**, *40*, 4422-4437. (b) Szymanski, W.; Beierle, J. M.; Kistemaker, H. A. V.; Velema, W. A.; Feringa, B. L. *Chem. Rev.* **2013**, *113*, 6114-6178.

[5] A. Bautista-Barrufet, M. Izquierdo-Serra, P. Gorostiza. Photoswitchable ion channels and receptors. In F. Benfenati et al. (eds.), Novel Approaches for Single Molecule Activation and Detection, Advances in Atom and Single Molecule Machines, DOI: 10.1007/978-3-662-43367-6_9, Springer-Verlag Berlin Heidelberg 2014.

[6] (a) Traynelis, S. F.; Wollmuth, L. P.; McBain, C. J.; Menniti, F. S.; Vance, K. M.; Ogden, K. K.; Hansen, K. B.; Yuan, H.; Myers, S. J.; Dingledine, R. *Pharmacol. Rev*. **2010**, *62*, 405-496. (b) Niswender, C. M.; Conn, P. J. *Annu. Rev. Pharmacol. Toxicol*. **2010**, *50*, 295-322.

[7] (a) Volgraf, M.; Gorostiza, P.; Numano, R.; Kramer, R. H.; Isacoff, E. Y.; Trauner, D. *Nat. Chem. Biol*. **2005**, *2*, 47-52. (b) Gorostiza, P.; Volgraf, M.; Numano, R.; Szobota, S.; Trauner, D.; Isacoff, E. Y. *Proc. Nat. Acad. Sci. USA* **2007**, *104*, 10865-10870.

[8] Kienzler, M. A.; Reiner, A.; Trautman, E.; Yoo, S.; Trauner, D.; Isacoff, E. Y. *J. Am. Chem. Soc*. **2013**, *135*, 17683-17686.

[9] Rullo, A.; Reiner, A.; Reiter, A.; Trauner, D.; Isacoff, E. Y.; Woolley, G. A. *Chem. Commun*. **2014**, *50*, 14613-14615.

[10] Yaroslavsky, A. N.; Schulze, P. C.; Yaroslavsky, I. V; Schober, R.; Ulrich, F.; Schwarzmaier, H. J. *Phys. Med. Biol.* **2002**, *47*, 2059–2073.

[11] Denk, W.; Strickler, J. H.; Webb, W. W. *Science* **1990**, *248*, 73-76.

[12] Papagiakoumou, E.; Begue, A.; Leshem, B.; Schwartz, O.; Stell, B. M.; Bradley, J.; Oron, D.; Emiliani, V. *Nat. Photon.* **2013**, *7*, 274-278.

[13] Oron, D.; Papagiakoumou, E.; Anselmi, F.; Emiliani, V. *Prog. Brain Res.* **2012**, *196*, 119-143.

[14] Watson, B. O.; Nikolenko, V.; Yuste, R. *Front. Neural Circuits* **2009**, *3*, 6.

[15] (a) De Boni, L.; Misoguti, L.; Zilio, S. C.; Mendonça, C. R. *ChemPhysChem* **2005**, *6*, 1121-1125; (b) Silva, D. L.; Krawczyk, P.; Bartkowiak, W.; Mendonça, C. R. *J. Chem. Phys.* **2009**, *131*, 244516.

[16] Izquierdo-Serra, M.; Gascón-Moya, M.; Hirtz, J. J.; Pittolo, S.; Poskanzer, K. E.; Ferrer, E.; Alibés, R.; Busqué, F.; Yuste, R.; Hernando, J.; Gorostiza, P. *J. Am. Chem. Soc*. **2014**, *136*, 8693-8701.

[17] Carroll, E. C.; Berlin, S.; Levitz, J.; Kienzler, M. A.; Yuan, Z.; Madsen, D.; Larsen, D. S.; Isacoff, E. Y. *Proc. Nat. Acad. Sci. USA* **2015**, *112*, E-776-E785.

[18] Blevins, A. A.; Blanchard, G. J. *J. Phys. Chem. B* **2004**, *108*, 4962-4968.

[19] Xu, C.; Williams, R. M.; Zipfel, W.; Webb, W. W. *Bioimaging* **1996**, *4,* 198–207.

[20] Chirico, G.; Cannone, F.; Baldini, G.; Diaspro, A. *Biophys. J.* **2003**, *84*, 588–598.

[21] Ezquerra, J.; Pedregal, C.; Rubio, A.; Yruretagoyena, B.; Escribano, A.; Sánchez-Ferrando, F. *Tetrahedron* **1993**, *49*, 8665-8678.

[22] Steger, M.; Young, D. W. *Tetrahedron* **1999**, *55*, 7935-7956.

[23] Pearson, R. J.; Kassianidis, E.; Slawin, A. M. Z.; Philp, D. *Org. Biomol. Chem*. **2004**, *2*, 3434-3441.

[24] Sousa, A. C.; Martins, L. O.; Robalo, M. P. *Adv. Synth. Catal*. **2013**, *355*, 2908-2917.

[25] Nishimura, N.; Sueyoshi, T.; Yamanaka, H.; Imai, E.; Yamamoto, S.; Hasegawa, S. *Bull. Chem. Soc. Japan* **1976**, *49*, 1381-1387.

[26] Kim, H. M.; Lee, Y. O.; Lim, C. S.; Kim, J. S.; Cho, B. R. *J. Org. Chem.* **2008**, *73*, 5127-5130.

[27] Kim, H. M.; Cho, B. R. *Acc. Chem. Res.* **2009**, *42*, 863-872.

[28] Lakowicz, J.R. Principles of Fluorescence Spectroscopy, Springer, NewYork, USA, **2006**.

[29] Berlman, I. B. Handbook of Fluorescence Spectra of Aromatic Molecules, Academic Press, New York and London, **1971**.

[30] Lees, A. J. *Anal. Chem.* **1996**, *68*, 226-229.

[31] Bandara, H. M. D.; Burdette, S. C. *Chem. Soc. Rev.* **2012**, *41*, 1809-1825.